



Hydroxyl radical scavenging by cerium oxide nanoparticles improves Arabidopsis salinity tolerance by enhancing leaf mesophyll potassium retention

Journal:	<i>Environmental Science: Nano</i>
Manuscript ID	EN-ART-03-2018-000323.R1
Article Type:	Paper
Date Submitted by the Author:	30-Apr-2018
Complete List of Authors:	Wu, Honghong; University of California, Riverside, Department of Botany and Plant Sciences Shabala, Lana; University of Tasmania, School of Land and Food Shabala, Sergey; University of Tasmania, Stress Physiology Giraldo, Juan Pablo; University of California, Riverside,

1
2
3 1 **Hydroxyl radical scavenging by cerium oxide nanoparticles improves *Arabidopsis* salinity**
4 **tolerance by enhancing leaf mesophyll potassium retention**
5
6
7 3

8 4 Honghong Wu¹, Lana Shabala², Sergey Shabala², Juan Pablo Giraldo^{1*}
9
10 5
11 6
12 7
13 8
14 8

15 8
16
17 9 **Environmental significance**
18

19 10 Environmental stresses, including salinity, lead to the accumulation of reactive oxygen species
20 11 (ROS) with subsequent damage to plant cellular components, reduced crop growth and yield.
21 12 Organisms lack enzymatic pathways for catalytically scavenging hydroxyl radicals, one of the
22 13 most destructive ROS, thus limiting the ability of molecular tools to manipulate this ROS *in vivo*.
23 14 Herein, we apply a nanobiotechnology-based approach that improves plant salinity stress
24 15 tolerance by scavenging hydroxyl radicals and its precursors. We determined the underlying
25 16 mechanisms of how cerium oxide nanoparticle (nanoceria) reduction of hydroxyl radical levels
26 17 in *Arabidopsis* leaves affects potassium fluxes across the plasma membrane. Nanoceria enable
27 18 higher retention of K⁺ in leaf mesophyll, thus improving plant photosynthetic performance and
28 19 biomass against environmental stress e.g. salinity.
29
30
31
32
33
34
35
36
37
38
39
40
41
42
43
44
45
46
47
48
49
50
51
52
53
54
55
56
57
58
59
60

1
2
3 1 **Hydroxyl radical scavenging by cerium oxide nanoparticles improves *Arabidopsis* salinity**
4 **tolerance by enhancing leaf mesophyll potassium retention**
5
6
7 3

8 4 Honghong Wu¹, Lana Shabala², Sergey Shabala², Juan Pablo Giraldo^{1*}
9

10 5
11
12 6 ¹ Department of Botany and Plant Sciences, University of California, Riverside, California
13 7 92521, U.S.

14
15 8 ² School of Land and Food, University of Tasmania, Hobart, Tasmania 7001, Australia
16

17 9 * Corresponding author: juanpablo.giraldo@ucr.edu, +1 9518273583
18
19
20
21
22
23
24
25
26
27
28
29
30
31
32
33
34
35
36
37
38
39
40
41
42
43
44
45
46
47
48
49
50
51
52
53
54
55
56
57
58
59
60

10 Abstract

11 Salinity is a widespread environmental stress that severely limits crop yield worldwide. Cerium
12 oxide nanoparticles (nanoceria) have the unique capability of catalytically reducing levels of
13 stress-induced reactive oxygen species (ROS) including hydroxyl radicals ($\cdot\text{OH}$) that lack
14 enzymatic scavenging pathways. The underlying mechanisms of how nanoceria ROS scavenging
15 augments plant tolerance to environmental stress are not well understood. Herein, we
16 demonstrate that catalytic $\cdot\text{OH}$ scavenging by nanoceria in *Arabidopsis thaliana* leaves
17 significantly improves mesophyll K^+ retention, a key trait associated with salinity stress
18 tolerance. Leaves with mesophyll cells interfaced with 50 mg/L poly (acrylic acid) coated
19 nanoceria (PNC) have significantly higher ($P < 0.05$) carbon assimilation rates (85 %), quantum
20 efficiency of photosystem II (9 %), and chlorophyll content (14 %) compared to controls after
21 being exposed to 100 mM NaCl for 3 days. PNC infiltrated leaves (PNC-Leaves) under salinity
22 stress exhibit lower ROS levels - including hydroxyl radical (41 %) and its precursor hydrogen
23 peroxide (44 %) - and one fold higher ($P < 0.05$) cytosolic K^+ dye intensity in leaf mesophyll
24 cells relative to controls. Non-invasive microelectrode ion flux electrophysiological (MIFE)
25 measurements indicated that PNC-Leaves have about three-fold lower NaCl-induced K^+ efflux
26 from leaf mesophyll cells compared to controls upon exposure to salinity stress. The ROS-
27 activated nonselective cation channels (ROS-NSCC) in the plasma membrane of leaf mesophyll
28 cells were identified as the main $\cdot\text{OH}$ -inducible K^+ efflux channels. Long term catalytic
29 scavenging of $\cdot\text{OH}$ in leaves by PNC enhances plant photosynthetic performance under salinity
30 stress by enabling plasma membrane channels/transporters to coordinately retain higher levels of
31 K^+ in the leaf mesophyll cell cytosol. PNC augmented plant ROS scavenging provides a key tool
32 for understanding and improving plant tolerance against abiotic stresses such as salinity.

33
34 **Keywords:** cerium oxide nanoparticles, hydroxyl radicals, ion channels and transporters, ion
35 fluxes, K^+ retention, salinity stress

1. Introduction

Salinity is a global issue threatening agricultural production in more than 50% irrigated land worldwide.^{1,2} Salt stress perturbs the equilibrium between reactive oxygen species (ROS) production and scavenging resulting in ROS accumulation with subsequent damage to proteins, lipids, carbohydrates, and DNA.^{3,4} Among several ROS - hydrogen peroxide, superoxide anion, hydroxyl radicals and singlet oxygen - hydroxyl radicals are the most destructive ROS and cannot be scavenged by any known enzymes in biological systems.^{3,5} Hydroxyl radicals ($\cdot\text{OH}$) have an extreme reactivity and a very short lifetime (~ 1 ns).⁶ These radicals are mainly generated in chloroplasts and mitochondria in plants under stress condition.^{3,4} They are produced by the Fenton reaction bio-synthesis pathway; a series of reactions that require H_2O_2 and transition metals as precursors.^{3,7} Genetic engineering approaches are not currently applicable for counteracting the damage directly caused by $\cdot\text{OH}$ in plants under abiotic stress. To the best of our knowledge, there are no reported methods to catalytically reduce $\cdot\text{OH}$ *in planta*.

Nanomaterials have distinct chemical, optical, and mechanical properties that can be applied as tools to study and engineer biological mechanisms in wild-type plants.⁸⁻¹² Cerium oxide nanoparticles (nanoceria) are potent catalytic scavengers of ROS including $\cdot\text{OH}$, hydrogen peroxide (H_2O_2), and superoxide anion.^{13,14} Nanoceria have a large number of surface oxygen vacancies that alternate between two oxidation states (Ce^{3+} and Ce^{4+}).¹⁵⁻¹⁷ The Ce^{3+} dangling bonds effectively scavenge ROS while the lattice strains at the nanoscale promote the regeneration of these defect sites via redox cycling reactions.¹⁸ Giraldo *et al.*⁸ showed that nanoceria (24 μM) catalytically scavenges both superoxide anion and hydrogen peroxide in isolated chloroplasts. Wu *et al.*¹⁹ reported that anionic nanoceria coated with poly (acrylic acid) (PNC, 51 mg/L) having low $\text{Ce}^{3+}/\text{Ce}^{4+}$ ratios significantly reduce ROS accumulation and improve photosynthetic performance in plants under abiotic stresses. Negatively charged nanoceria are more efficiently delivered to chloroplasts than their positively charged counterparts. Furthermore, low $\text{Ce}^{3+}/\text{Ce}^{4+}$ ($\sim 35\%$) nanoceria have catalase (CAT) and super oxide dismutase (SOD) mimetic activity in plants.^{16,19}

The study of plant-nanoceria interactions has mainly focused on nanoceria uptake and distribution,²⁰⁻²⁴ and the effect of nanoceria on antioxidant enzyme activities,^{25,26} photosynthetic

1
2
3 67 performance,^{27,28} and abiotic stress tolerance^{19,29}. Recently, we reported that negatively charged
4 68 nanoceria (10 ± 1.3 nm, ~ 50 mg/L) augment ROS scavenging and photosynthetic performance
5 69 of *Arabidopsis* plants under high light, heat, and dark chilling.¹⁹ Similarly, previous studies have
6 70 shown that anionic nanoceria enhance photosynthetic rates in soybean (100 mg/Kg) (*Glycine*
7 71 *max* L. Merr.)²⁸ and increase shoot biomass in carrot (50 mg/Kg) (*Daucus carota* cv. Danvers
8 72 Half Long).²⁰ Negatively charged nanoceria (200-1000 mg/Kg) applied to soil also improve net
9 73 photosynthetic rates and leaf biomass in canola (*Brassica napus* cv. Dwarf Essex) exposed to salt
10 74 stress (100 mM NaCl).²⁷ The underlying mechanisms of how nanoceria ROS scavenging
11 75 improves plant tolerance to environmental stress such as salinity are not well understood. It has
12 76 been shown that mesophyll K⁺ retention is a key trait conferring plant salt tolerance,³⁰⁻³² mainly
13 77 controlled by K⁺ efflux from the cytosol to the apoplast. The plasma membrane K⁺-selective
14 78 (GORK) and non-selective (NSCC) cation efflux channels mediate K⁺ retention in plants under
15 79 salt stress.³³ Hydroxyl radicals are known to activate GORK in *Arabidopsis* roots³⁴ and ROS-
16 80 activated NSCC channels^{35,36}. How hydroxyl radicals affect leaf mesophyll K⁺ retention under
17 81 salinity stress is unclear. Herein, we study the mechanisms of how anionic nanoceria (PNC) *in*
18 82 *vivo* scavenging of [•]OH in leaves impacts plant performance under salinity stress.

19 83
20 84 Using a plant nanobiotechnology approach we enabled wild-type *Arabidopsis* plants with
21 85 augmented scavenging of ROS including [•]OH by embedding PNC in leaf mesophyll tissues. We
22 86 hypothesized that catalytic [•]OH scavenging by PNC modulates the activities of K⁺ efflux
23 87 channels and reduces NaCl-induced K⁺ efflux from leaf mesophyll cells improving salinity stress
24 88 tolerance. To assess plant performance under salt stress, we measured chlorophyll content index,
25 89 shoot biomass, and key light and carbon reaction of photosynthesis parameters. We also
26 90 quantified PNC ability for *in vivo* scavenging of [•]OH and its impact on mesophyll K⁺ retention.
27 91 To elucidate the mechanisms of PNC action on mesophyll K⁺ retention, we measured changes in
28 92 leaf plasma membrane K⁺ channel activity and gene expression.

29 93 30 94 **2. Materials and Methods**

31 95 **2.1. Plant material**

32 96 Four weeks old *Arabidopsis thaliana* (Columbia 0) plants were grown in pots (2 x 2 inch, 32
33 97 inserts) filled with standard soil mix (Sunshine, LC1 mix). After one-week germination one

1
2
3 98 individual seedling was kept in each pot. Plants were grown in Adaptis 1000 growth chamber
4
5 99 (Conviron) at $200 \mu\text{mol m}^{-2} \text{s}^{-1}$ photosynthetic active radiation (PAR), $24 \pm 1 \text{ }^\circ\text{C}$ and $21 \pm 1 \text{ }^\circ\text{C}$ at
6
7 100 day- and night- time, respectively. Relative humidity was maintained at 60 %, and day/night
8
9 101 regime was 14h/10 h. Plants were hand-watered with deionized water once every two days.

10
11

12 103 **2.2. Synthesis and characterization of PNC**

13 104 Low $\text{Ce}^{3+}/\text{Ce}^{4+}$ ratio cerium oxide nanoparticles (nanoceria) coated with poly (acrylic acid) (PNC)
14
15 105 were synthesized and characterized as described in Wu *et al.*¹⁹ Briefly, 1.08 g cerium (III) nitrate
16
17 106 (Sigma Aldrich, 99%) and 4.5 g poly (acrylic acid) (1,800 MW, Sigma Aldrich) were dissolved
18
19 107 in 2.5 mL and 5.0 mL molecular biology grade water (Corning, Mediatech, Inc.), respectively.
20
21 108 The solutions were mixed thoroughly at 2,000 rpm for 15 min using a vortex mixer and added
22
23 109 dropwise to a 50 mL beaker containing 15 mL, 30% ammonium hydroxide solution (Sigma
24
25 110 Aldrich). The mixture was stirred at 500 rpm for 24 h at ambient temperature, then centrifuged at
26
27 111 4,000 rpm for 1 h to remove any debris and large agglomerates. The supernatant was purified
28
29 112 from free polymers and other reagents by centrifugation at 4,500 rpm (Allegra X30, Beckman)
30
31 113 using a 10K Amicon cell (MWCO 10K, Millipore Inc.) for at least six cycles (15 min each cycle).
32
33 114 After each cycle, the eluent absorption spectrum was measured in a UV-VIS spectrophotometer
34
35 115 (UV-2600, Shimadzu) until no peaks of free polymers and other reagents were detected. The
36
37 116 purified PNC suspension was filtered through a 20 nm pore size syringe filter (Whatman,
38
39 117 AnotopTM 25). The final PNC solution was stored in a refrigerator ($4 \text{ }^\circ\text{C}$) until further use.

118

119 The concentration of the final PNC solution was calculated from the absorption spectrum
120
121 measured by the UV-VIS spectrophotometer (UV-2600, Shimadzu) (Fig. S1A) using Beer-
122
123 Lambert's law ($A = \epsilon CL$) with absorbance at 271 nm, absorption molar coefficient (ϵ) of 3 cm^{-1}
124
125 mM^{-1} ,³⁷ and pathway length (L) of 1 cm. C is the molar concentration of the measured sample.
126
127 Sample concentration in mg/L was calculated by using the molecular weight of cerium (III)
128
129 oxide and cerium (IV) oxide weighted by the $\text{Ce}^{3+}/\text{Ce}^{4+}$ ratios for PNC. Pulido-Reyes *et al.*¹⁶
130
131 showed that negligible amounts of dissolved Ce (ranging from 0.00001 to 0.0008 mg/l) in
132
133 different types of nanoceria (10 mg/L). No dissolved $\text{Ce}(\text{NO}_3)_3$ absorption peaks were found in
134
135 purified PNC solution.¹⁹ Molecular grade water was used to determine that the resolution of
136
137 absorbance values collected by the UV-VIS spectrophotometer is less than 0.01.

1
2
3 129
4
5 130 The hydrodynamic diameter (DLS size) and zeta potential of synthesized PNC are 10 ± 0.6 nm
6
7 131 and -17 ± 2.7 mV, respectively. Four separate measurements were conducted. The zeta potential
8
9 132 and size of PNC in solution were measured by a Malvern Zetasizer (Nano ZS) (resolution < 0.1
10
11 133 mV) and Sizer (Nano S) (resolution < 0.1 nm, detection limit: 0.3 nm), respectively. Fourier
12
13 134 transformed infrared spectroscopy (FTIR) was performed with Nicolet 6700 FTIR (Thermo
14
15 135 Electron Corp.) to confirm the presence of $-\text{COOH}$ group in PNC (Fig. S1B). Dried PNC
16
17 136 powder were used and the background was collected and subtracted accordingly. The $\text{Ce}^{3+}/\text{Ce}^{4+}$
18
19 137 ratio measured by XPS is 35 ± 2.2 % (Fig. S1C). Dry samples of PNC were mounted on a carbon
20
21 138 tape for XPS (X-ray photoelectron spectroscopy, Kratos Axis Ultra X-ray Photoelectron
22
23 139 Spectroscopy) measurement to characterize the ratio of the Ce^{3+} and Ce^{4+} .
24

24 141 **2.3. *In vitro* assay of nanoceria scavenging of hydroxyl radical**

25
26 142 The ability of nanoceria to scavenge hydroxyl radicals was tested *in vitro*. Here Cu/Asc
27
28 143 (copper/sodium ascorbate) and HPF (hydroxyphenyl fluorescein) dye were used. Cu/Asc mixture
29
30 144 generates hydroxyl radicals. HPF remains in non-fluorescent form until it reacts with $\cdot\text{OH}$ or
31
32 145 peroxy nitrite anion. Thus, the hydroxyl radical scavenging ability of PNC can be monitored by
33
34 146 measuring the decrease of fluorescence of HPF in the presence of hydroxyl radicals. First, 71.5
35
36 147 μl HPF dye (10 μM , in TES infiltration solution) was transferred into each well (Costar white 96
37
38 148 well microplate with flat bottom, Corning). Then 10 μl ascorbate sodium solution (10 mM, in
39
40 149 ddH₂O) and 8.5 μl PNC (5.4 mM, in ddH₂O) added. A solution (10 μl) of copper chloride (3 mM,
41
42 150 in ddH₂O) was added into each well and the fluorescence of HPF dye was measured immediately
43
44 151 using Victor 2 plate reader (Wallac) at 485/530 nm (excitation/emission) for 15 min. Final PNC
45
46 152 concentration in this reaction mixture is 50 mg/L, the same concentration used *in vivo*. A
47
48 153 concentration of 50 mg/L PNC was previously determined to be optimal for augmenting plant
49
50 154 ROS scavenging and enhancing photosynthesis under abiotic stress in *Arabidopsis*.¹⁹ The
51
52 155 fluorescence of reaction system without PNC was used as control. To avoid any possible
53
54 156 confounding effects, the fluorescence was also measured in HPF alone and also the combination
55
56 157 of HPF + CuCl₂, HPF + Na-Ascorbate and HPF + PNC were tested. The ability of PNC with a
57
58 158 low $\text{Ce}^{3+}/\text{Ce}^{4+}$ ratio to scavenge superoxide anion and hydrogen peroxide was shown previously
59
60 159 by Wu *et al.*¹⁹

160

161 **2.4. Nanoceria leaf infiltration**

162 Leaves were slowly infiltrated with nanoceria through the leaf abaxial side with ~200 μL of
163 solution (50 mg/L ¹⁹ PNC in 10 mM TES infiltration buffer) by gently pressing the tip of the
164 syringe (NORM-JECT®, 1 ml) against the leaf lamina. A 10 mM TES infiltration buffer solution
165 (10 mM TES, 10 mM MgCl_2 , pH 7.5) was used as control. Kimwipes were used to gently
166 remove the excess solution remaining on the surface of leaf lamina. Infiltrated plants were kept
167 on the bench under light for leaf adaptation and incubation with nanoceria for 3 h. A detailed
168 protocol for leaf lamina infiltration of nanoparticles is given in *Wu et al.*³⁸

169

170 **2.5. Leaf chlorophyll content**

171 Chlorophyll content index (CCI) was monitored in wild-type *Arabidopsis* plants infiltrated with
172 PNC and buffer solution (controls) for 3 days after onset of the salinity stress (100 mM NaCl).
173 Four week old plants infiltrated with PNC or buffer as explained above were randomly
174 distributed in 1020 greenhouse trays without holes filled with 100 mM NaCl (a commonly used
175 NaCl concentration for *Arabidopsis* salinity stress studies³⁹⁻⁴¹). CCI measurements were
176 performed using a chlorophyll meter (SPAD-502 plus, Konica Minolta, Tokyo, Japan; CCI
177 readout resolution: 0.1) with each leaf being measured three times (each time/data point was
178 composed of at least three CCI readout).

179

180 **2.6. Shoot biomass**

181 Shoot biomass was monitored in PNC- and buffer- infiltrated *Arabidopsis* plants after two weeks
182 of salt stress (100 mM NaCl). Four week old plants infiltrated with PNC or buffer as explained
183 above were randomly distributed in 1020 greenhouse trays without holes filled with 100 mM
184 NaCl. After salt treatment, the above ground plant biomass was collected and weighted
185 immediately. Then, samples were dried in oven at 65 °C for 72 h and dry weight was recorded.

186

187 **2.7. Leaf gas exchange and chlorophyll fluorescence**

188 Gas exchange and chlorophyll fluorescence measurements were performed in *Arabidopsis* leaves
189 from four week old plants exposed to 3 days of 100 mM NaCl using a GFS-3000 (Walz) as
190 described in *Wu et al.*¹⁹ Leaves larger than the gas analyzer chamber (2.5 x 1 cm^2) and with

1
2
3 191 similar chlorophyll content index were infiltrated with TES infiltration buffer (control) and PNC
4 192 (50 mg/L PNC in 10 mM TES infiltration buffer) and incubated for 3 h under room conditions.
5
6 193 Leaves were dark adapted for 10 min before Fv/Fm measurements. A-light curve was performed
7
8 194 at decreasing light levels from 900, 600, 400, 300, 200, 100, 50 to 0 $\mu\text{mol m}^{-2} \text{s}^{-1}$ PAR. The GFS
9
10 195 cuvette temperature was set at 23 °C and 50 % relative humidity.
11
12 196

13 197 **2.8. DAB and NBT staining**

14
15 198 DAB (3,3'-diaminobenzidine) and NBT (nitro blue tetrazolium) staining was performed
16
17 199 following the protocol by Kumar *et al.*⁴² with modifications. DAB (50 mg) and NBT (100 mg)
18
19 200 were dissolved in 50 ml ddH₂O (pH adjusted to 3.8 by HCl) and 50 ml sodium phosphate buffer
20
21 201 (50 mM, pH 7.5), respectively. Leaves of salt treated plants were excised and placed in 50 ml
22
23 202 falcon tubes (wrapped with aluminum foil) with either freshly prepared DAB or NBT solutions
24
25 203 and kept overnight at ambient temperature. Then staining solutions were removed and 40 ml of
26
27 204 absolute ethanol was added. Samples were placed into a boiling water bath for 15 to 20 min and
28
29 205 periodically shaken. Ethanol was removed and leaves placed on a paper towel saturated with 60 %
30
31 206 glycerol. Pictures were taken with a Nikon Coolpix S7000 camera.
32

33 208 **2.9. *In vivo* ROS scavenging by nanoceria**

34 209 Leaf discs (~5 mm diameter) from the PNC and buffer infiltrated plants (four weeks old) were
35
36 210 incubated with either 25 μM 2',7'-dichlorodihydrofluorescein diacetate (H₂DCFDA, Thermo
37
38 211 Fisher Scientific), 10 μM dihydroethidium (DHE, Thermo Fisher Scientific) or 10 μM
39
40 212 hydroxyphenyl fluorescein (HPF, Thermo Fisher Scientific) dyes (in TES infiltration buffer, pH
41
42 213 7.5) in 1.5 mL Eppendorf tubes for 30 min under darkness. Incubated samples were mounted on
43
44 214 microscope slides inside a well formed by observation gel (Carolina, item 132700) filled with
45
46 215 PFD (perfluorodecalin). A coverslip was placed on the top to seal the well ensuring that no air
47
48 216 bubbles remain trapped under. The samples were imaged by a Leica SP5 confocal microscope
49
50 217 (Leica Microsystems, Germany). Confocal imaging settings were: 40x wet objective; 496 nm
51
52 218 laser excitation; Line average: 4; PMT1: 500-600 nm; PMT2: 700-800 nm. Three to eight
53
54 219 individual assessments (4 leaf discs for each plant) were done. The microscope was manually
55
56 220 focused on a region of leaf mesophylls cells. The fluorescence signal from the ROS dyes was
57
58 221 collected and recorded. Z-stacks ("xyz") of two different regions were taken per leaf disc. Z-

1
2
3 222 Stack section thickness of 2 μm ; 16 layers per leaf disc. DHE, DCF and HPF fluorescence
4
5 223 intensity was measured and analyzed in Image J within the imaged region of spongy mesophyll
6
7 224 cells using ImageJ software (NIH).

8
9 225

10 226 **2.10. Live imaging of K^+ distribution in mesophyll cells**

11 227 Imaging of K^+ distribution in the cytosol and vacuole was performed using 20 μM of the K^+ dye
12 228 APG-2 AM (asante potassium green-2AM, Abcam Biotechnology company) and 20 μM of FM
13 229 4-64 (*N*-(3-triethylammoniumpropyl)-4(6-(4-(diethylamino) phenyl) hexatrienyl) pyridinium
14 230 dibromide, Thermo Fisher Scientific) for plasma membrane and tonoplast staining. The
15 231 fluorescent dyes were dissolved in pure DMSO and diluted with TES infiltration buffer to
16 232 working concentration. Leaves of 4 week old *Arabidopsis* plants treated with 100 mM NaCl for 3
17 233 days were collected and the epidermis peeled off. Leaf discs were incubated with APG-2 AM
18 234 and FM-4-64 dyes in 1.5 mL Eppendorf tubes for 2.5 h in darkness. After incubation, leaf discs
19 235 were rinsed in ddH₂O and mounted on microscope slides for confocal imaging. The confocal
20 236 imaging settings were: 488 nm laser excitation (30 %); PMT1: 520-560 nm; PMT2: 610-630 nm.
21 237 Z-stacks (“xyz”) measurement were taken per leaf disc with Z-Stack section thickness of 2 μm ;
22 238 16 layers per leaf disc. The layer with strongest fluorescence intensity with APG-2 fluorescence
23 239 was analyzed by ImageJ software (NIH). The background values were deducted from analysis.
24 240 Three to five individuals (4 leaf discs for each plant) in total were used for these experiments.

25
26
27
28
29
30
31
32
33
34
35
36 241

37 242 **2.11. Mesophyll cell K^+ and H^+ flux measured by MIFE**

38 243 Net K^+ and H^+ fluxes were measured from leaf segments using non-invasive microelectrode ion
39 244 flux estimation technique (the MIFE^{43,44}). Blank microelectrodes were pulled out from
40 245 borosilicate glass capillaries (GC 150-10; Harvard Apparatus, Kent, UK) and dried overnight at
41 246 225 °C in an oven. The blank microelectrodes were then silanized with tributylchlorosilane (No
42 247 282707, Sigma-Aldrich). After drying and cooling, electrode blanks were back filled with
43 248 appropriate backfilling solutions (200 mM KCl for K^+ ; 15 mM NaCl + 40 mM KH_2PO_4 , pH
44 249 adjusted to 6.0 for H^+ microelectrodes). Then the tips of respective microelectrodes were front
45 250 filled with commercially available selectophore cocktails (Cat. No 60031 for K^+ or Cat. No
46 251 95297 for H^+ , Sigma-Aldrich). Microelectrodes were mounted in MIFE electrode holders and
47 252 calibrated in sets of appropriate standard solutions (see Shabala *et al.*⁴³ for methodological

1
2
3 253 details). Only microelectrodes with a slope over 50 mV per decade and correlation over 0.999
4 254 were used. Leaf segments were cut angularly to expose mesophyll cells and mounted in holders
5 255 and preconditioned in BSM solution for 0.5 h. Calibrated microelectrodes were co-focused and
6 256 aligned with a leaf sample and the electrode tips positioned 40 μm from the exposed mesophyll
7 257 surface. During measurements, a computer-controlled stepper motor moved electrodes in a 6-s
8 258 square-wave cycle between two positions, 40 and 110 μm above the exposed mesophyll surface.
9 259 The recorded electrochemical gradient potential change was converted into net ion fluxes changes
10 260 using the calibrated values of the ion selective microelectrodes and cylindrical diffusion
11 261 geometry of the exposed mesophyll area (MIFEFLUX software^{43,44}). At least four leaf segments
12 262 from different plants were assessed.
13
14
15
16
17
18
19
20
21

263

264 **2.12. Pharmacological experiments**

265 The identity of K^+ transport systems underlying hydroxyl radicals-induced K^+ efflux from
266 *Arabidopsis* mesophyll cells was investigated in a series of pharmacological experiments using
267 some known ion channel blockers. For K^+ flux experiments, leaf samples of control plants were
268 pre-treated for 1 h with either 20 mM tetraethyl ammonium chloride (TEA^+ , a known blocker of
269 K^+ selective channels³²) or 0.1 mM gadolinium chloride (Gd^{3+} , a known blocker of NSCC
270 channels³²). Steady-state K^+ fluxes were recorded over a period of 5 min. Then, Cu/Asc (0.3
271 mM/1 mM) mixture was administered to the measuring chamber and kinetics of net K^+ fluxes
272 recorded for a further 20 min. All chemicals used were from Sigma-Aldrich.
273

274

275 **2.13. Plasma membrane potential measurement**

276 Conventional KCl-filled Ag/AgCl microelectrodes with tip diameter 0.5 μm were used to
277 measure the plasma membrane potential (MP) of *Arabidopsis* leaf segments. Measurements were
278 taken from at least five individual plants for each treatment. MPs were recorded for at least 10
279 secs after the potential stabilized following cell penetration.
280

281

282 **2.14. Leaf K^+ content estimation**

283 0.3 g dry leaf samples were digested in a 120-ml Teflon digestion vessel with 5ml HNO_3 by
284 using a microwave digester (Mars 6 Microwave Digestion System, CEM Corporation, Matthews,
285 NC, USA). Digested samples were centrifuged at 5,000 g for 10 min at ambient temperature
286
287
288
289
290

1
2
3 284 (Avanti J-30I centrifuge, Beckman Coulter, Krefeld, Germany). After centrifugation, 0.2 mL of
4
5 285 the digested solution was diluted with ddH₂O to a final volume of 10 ml. K⁺ content was then
6
7 286 measured using a Flame Photometer (PFP7, Jenway, UK).
8
9 287

10 288 **2.15. ATP content determination**

11 289 Leaf ATP content of plants infiltrated with PNC or buffer was measured using ATP content
12 290 determination kit (A22066, Thermofisher). Extraction of leaf ATP was conducted by following
13 291 previously used methods with some modifications.^{45,46} Briefly, about 0.1 g leaf sample from PNC
14 292 or buffer infiltrated plants was grinded with liquid nitrogen by using mortar and pestle. The
15 293 sample was transferred to a 1.5 ml Eppendorf tube and 1 ml HCl (0.1 M) added and mix
16 294 thoroughly and put into boiling water for 10 min. After cooling down on ice, samples were
17 295 centrifuged at 16, 000 rpm for 3 min, and the transferred supernatant was centrifuged again. ATP
18 296 measuring reaction solution (containing 20X reaction buffer, 0.1 M DTT, 10 mM D-luciferin,
19 297 and 5 mg/ml firefly luciferase) was mixed according to manufacturer's instruction. The 90 µl
20 298 reaction solution was added into each well (Costar white 96 well microplate with flat bottom,
21 299 Corning). Then, 10 µl diluted ATP standard solutions or leaf sample solution were added into
22 300 each well. Luminescence (emission 560 nm) was measured with Victor 2 plate reader (Wallac)
23 301 immediately according to manufacturer's protocol.
24
25
26
27
28
29
30
31
32
33

34 302

35 303 **2.16. Quantitative real-time PCR analysis**

36 304 PNC-leaves and NNP-leaves from four weeks old *Arabidopsis* (Col-0) plants exposed to 3 days
37 305 100 mM NaCl were excised, cut into small segments, and snap frozen in liquid nitrogen. The leaf
38 306 RNA was extracted and synthesized to cDNA by using AurumTM Total RNA Mini Kit (Bio-Rad)
39 307 and iScript RT supermix (one-step cDNA mix, Bio-Rad) following the manufacture's instruction
40 308 ⁴⁷. Quantitative real-time PCR was performed using a Bio-Rad CFX Connect Real Time Thermal
41 309 Cycler and SYBR green PCR reagent (Bio-Rad) as described in Vandesompele *et al.*⁴⁸ The
42 310 relative expression level of studied genes was analyzed by $2^{-\Delta\Delta C_T}$ method.⁴⁹ Primers were
43 311 designed to determine the expression of *AtGork*,⁵⁰ *AtHAK5*,⁵¹ *AtAVP*,⁵² *AtNHX1*⁵² and *ATAHAI*⁵²
44 312 (see Suppl. Table S1 for primer sequences). The control gene (*Actin*⁵³ and *GAPDH*⁵⁴) was used
45 313 for normalization of the test gene transcript. Experiments were repeated in three individuals
46 314 (each biological replicate was measured for four times).
47
48
49
50
51
52
53
54
55
56
57
58
59
60

315

2.17. Statistical analysis

All data were represented as mean \pm SE (n = biological replicates) and analyzed using SPSS 23.0. Comparison was performed by independent samples *t*-test (two tailed) or one-way ANOVA based on Duncan's multiple range test (two tailed). *, **, and *** represent $P < 0.05$, $P < 0.01$ and $P < 0.001$, respectively. Different lower case letters mean the significance at $P < 0.05$.

321

3. Results and Discussion

The underlying mechanisms of how nanoceria catalytic ROS scavenging affects plant physiological processes associated with salinity stress tolerance are not well understood. Herein, we determined that sub 11 nm negatively charged nanoceria improve chlorophyll content, biomass, photosynthesis, and leaf mesophyll K^+ retention in *Arabidopsis* plants under salt stress. We show that PNC catalytic scavenging of hydroxyl radical and its precursor hydrogen peroxide enables higher mesophyll K^+ retention in leaves of plants under salt stress by affecting the activity and gene expression of K^+ channels/transporters (Fig. 1). Leaf mesophyll K^+ retention has been associated with overall salinity stress tolerance in plants.^{32,55} K^+ is an essential nutrient for plants that plays an important role in protein synthesis stabilization, enzyme activation, membrane potential formation and maintenance of turgor pressure.³¹

333

3.1. Enhanced salinity tolerance in *Arabidopsis* plants engineered with nanoceria

Plant tolerance to salt stress was assessed by measuring changes in plant agronomical (shoot biomass) and physiological parameters (chlorophyll content; leaf photosynthetic traits). After three days of 100 mM NaCl, plants infiltrated with PNC were visibly healthier (Fig. 2A) and exhibited higher chlorophyll content levels relative to controls infiltrated with buffer with no nanoparticles (NNP) (SPAD readout, Fig. 2B). We observed enhanced photosystem II quantum yield (QY, up to 30 % increase, $P < 0.05$) (Fig. 2C) and higher maximum efficiency of photosystem II (Fv/Fm, 9 %, $P < 0.05$, Fig. 2D) in leaves infiltrated with PNC (PNC-leaves) relative to their control counterparts without nanoparticles (NNP-leaves). No significant differences in either chlorophyll content index, QY, and Fv/Fm were found between PNC-leaves and NNP-leaves under non-saline conditions (Fig. S2). The salt stressed PNC-leaves have increased carbon assimilation rates (A, 85 %, $P < 0.05$) (Fig. 2E) and quantum efficiency of CO_2

1
2
3 346 (ϕCO_2 , 26 %, $P < 0.05$) (Fig. 2F) compared to NNP-leaves. These changes in leaf carbon uptake
4
5 347 were accompanied by higher stomatal conductance (Gs) in PNC-leaves (up to 38 % increase, $P <$
6
7 348 0.05) relative to NNP-leaves under salt stress (Fig. S3). Negatively charged PNC (51 mg/L)
8
9 349 exhibit high levels of colocalization with *Arabidopsis* leaf mesophyll chloroplasts *in vivo* (46 %)
10
11 350 where they enhance photosynthesis under abiotic stress by scavenging ROS.¹⁹ PNC also improve
12
13 351 shoot biomass (18 %, $P < 0.05$) in four-week-old plants subjected to 100 mM NaCl for two
14
15 352 weeks, relative to plants without nanoparticles (Fig. S4). Our results are in agreement with a
16
17 353 previous study showing that negatively charged nanoceria (zeta potential -51.8 mV, average
18
19 354 TEM size 55.6 nm, 1000 mg/Kg) applied to soil alleviates salt stress induced symptoms
20
21 355 including reduced leaf biomass, total chlorophyll content, and net carbon assimilation rates in
22
23 356 canola plants.²⁷ In contrast, plant exposure to cerium in the ionic form in $\text{Ce}(\text{SO}_4)_2$ (0.5-500
24
25 357 mg/L)²⁰ or CeCl_3 (10 mg/L)⁵⁶ decreases or has no significant effect on root and shoot biomass.
26
27 358 Nanoceria ability to regenerate Ce^{3+} dangling bonds and catalytically scavenge ROS provides
28
29 359 *Arabidopsis* plants with sustained alleviation of oxidative stress and enhancement in
30
31 360 photosynthetic performance under salt stress.

361

362 **3.2. ROS catalytic scavenging by nanoceria in salinity stressed leaves**

363 ROS accumulation is a hallmark of abiotic stress in plants. Hydroxyl radical generation *in vivo*
364
365 was monitored via confocal fluorescence microscopy with HPF (hydroxyphenyl fluorescein) dye.
366
367 HPF remains in a non-fluorescent form until it reacts with $\cdot\text{OH}$ or peroxyxynitrite anion but not
368
369 other ROS.⁵⁷ The high HPF selectivity of 6:1 between $\cdot\text{OH}$ and peroxyxynitrite⁵⁷ has been used for
370
371 *in vivo* imaging of $\cdot\text{OH}$ in mammalian cells.⁵⁸ We conducted *in vitro* nanoceria ROS scavenging
372
373 experiments that demonstrated PNC effectively reduces levels of $\cdot\text{OH}$ generated by Cu/Asc as
374
375 indicated by the significantly lower fluorescence intensity of HPF dye in samples with PNC
376
377 relative to buffer without nanoparticles (Fig. 3A). We report a significantly lower HPF dye
378
379 fluorescence (41 %, $P < 0.001$) in PNC-Leaves relative to NNP-Leaves under salt stress (Fig.
380
381 3C and 3D) indicating efficient scavenging of $\cdot\text{OH}$ in salt stressed plants by PNC *in vivo*.
382
383 Hydrogen peroxide, a precursor of $\cdot\text{OH}$, was visualized by histochemical staining with DAB
384
385 (3,3'-diaminobenzidine) of PNC-leaves and NNP-leaves (Fig. 3B). DAB staining clearly showed
386
387 lower accumulation of H_2O_2 in PNC-leaves than in NNP-leaves after 3 days of salt stress (100
388
389 mM NaCl). Confocal imaging of H_2O_2 was conducted using H_2 -DCFDA (2',7'-

1
2
3 377 dichlorodihydrofluorescein diacetate) dye. DCFDA reaction with ROS, primarily with H₂O₂,
4 378 leads to conversion into its fluorescent form DCF (2',7'-dichlorofluorescein). DCF fluorescence
5
6 379 intensity in PNC-leaves is 44 % lower than that of NNP-leaves after 3 days of salt stress ($P <$
7
8 380 0.001) (Fig. 3B, 3C, and 3E). NBT (nitro blue tetrazolium chloride) staining and DHE
9
10 381 (dihydroethidium) dye were applied to image superoxide anion (Fig. S5A), a precursor of H₂O₂.
11
12 382 DHE can freely permeate cell membranes and react with superoxide anions to generate its
13
14 383 fluorescent form 2-hydroxyethidium.⁵⁹ PNC-leaves have 37 % less ($P < 0.01$) DHE fluorescence
15
16 384 intensity than NNP-leaves after salt stress (Fig. S5B and S5C). Nanoceria *in vitro* scavenging of
17
18 385 superoxide anion and H₂O₂ has been previously reported.^{16,19} The PNC used in this study have
19
20 386 low Ce³⁺/Ce⁴⁺ ratio ($35 \pm 2.2\%$) (Fig. S1) which has been identified as having CAT and SOD
21
22 387 mimetic activity that effectively scavenges ROS.^{16,19} Overall, our results demonstrate that PNC
23
24 388 significantly lower levels of $\cdot\text{OH}$ and its precursor H₂O₂ in leaves of *Arabidopsis* plants under
25
26 389 salt stress.

390

391 **3.3. Higher K⁺ retention in leaf mesophyll cells with embedded nanoceria**

392 Leaf mesophyll K⁺ distribution in the vacuole and cytosol was imaged using APG-2 cell
393 permeable fluorescent dye together with FM4-64 for plasma membrane and tonoplast staining.
394 Under salt stress, PNC-leaves exhibit an almost one-fold higher K⁺ dye intensity in the cytosol
395 than NNP-leaves (Fig. 4A and 4B) and K⁺ content in whole PNC-Leaves is higher than in NNP-
396 Leaves (Fig. 4C) indicating that PNC ROS scavenging promotes K⁺ mesophyll retention in
397 leaves. No differences in leaf K⁺ content were found between plants infiltrated with PNC and
398 buffer solution under control conditions (Fig. 4C). The K⁺ dye intensity values were similar in
399 the vacuole of leaf mesophyll cells under salt stress (Fig. 4B). To date, no ROS activated
400 vacuolar K⁺ channels or transporters have been reported in leaf mesophyll cells⁶⁰, in agreement
401 with the lack of differences in vacuole K⁺ levels between PNC-Leaves and NNP-Leaves. Non-
402 invasive microelectrode ion flux estimation (MIFE) measurements found that both transient and
403 steady-state NaCl-induced K⁺ efflux is higher in NNP-leaves than in PNC-leaves (Fig. 5A). Thus,
404 PNC-leaves have a significantly less K⁺ loss than NNP-leaves under salt stress (Fig. 5B). In
405 contrast, no significant differences of NaCl-induced H⁺ flux and average H⁺ loss were observed
406 between PNC-leaves and NNP-leaves (Fig. 5C and 5D). Plasma membrane potential is a key
407 plant physiological trait that influences the transport of ions across the cell membrane.^{33,43,61–65}

1
2
3 408 This potential is mainly built by H^+ -ATPase pumping of H^+ from cytosol to the apoplast.⁶⁶ One
4 409 of the detrimental effects of salinity stress is the depolarization of the plasma membrane
5 410 potential.^{32,67,68} Our results indicate that although PNC enhances K^+ mesophyll retention it does
6 411 not affect the plasma membrane potential in *Arabidopsis* plants under salt stress.
7
8
9

10 412
11
12 413 The effect of nanoparticles e.g. nanoceria on the activity of plasma membrane
13 414 channels/transporters controlling K^+ fluxes is poorly understood. Recently, Sosan *et al.*⁶⁹ found
14 415 that silver nanoparticles slightly inhibit plasma membrane K^+ efflux currents in *Arabidopsis* root
15 416 cell protoplasts. We measured K^+ fluxes in PNC- and NNP-inoculated leaves in response to ROS
16 417 accumulation, a secondary stress in plants under high salinity.⁷⁰ Hydroxyl radicals were
17 418 generated by copper/ascorbate (Cu/Asc) mixture and the effect of H_2O_2 (30%, Sigma Aldrich)
18 419 was also tested. A 48 % and 45 % lower K^+ efflux was observed in PNC-leaves relative to NNP-
19 420 leaves in the presence of $\cdot OH$ (Cu/Asc solution) (Fig. 6A and 6C) and in samples treated with
20 421 H_2O_2 , respectively (Fig. 6B and 6C) ($P < 0.001$). ROS-activated NSCC channel activity can be
21 422 promoted in the presence of $\cdot OH$ or H_2O_2 . However, the K^+ efflux induced by $\cdot OH$ is over ten
22 423 times higher than that induced by H_2O_2 (Fig. 6A-C). A high K^+ efflux has also been reported in
23 424 *Arabidopsis* roots in the presence of $\cdot OH$ (generated by Cu/Asc).⁷¹ Hydrogen peroxide, a
24 425 precursor of $\cdot OH$, also stimulates K^+ efflux in *Arabidopsis* roots likely by reacting with transition
25 426 metals to form $\cdot OH$.³⁴ Furthermore, samples pretreated with Gd^{3+} , a blocker for NSCC, showed
26 427 over 90 % blockage of $\cdot OH$ induced K^+ efflux in leaf mesophyll cells (Fig. 6D and 6E).
27 428 Application of TEA (tetraethylammonium), a GORK channel inhibitor, was much less efficient
28 429 (~ 50 % inhibition of K^+ efflux in the presence of $\cdot OH$) (Fig. 6D). However, both plasma
29 430 membrane potential depolarization (gating factors that trigger GORK channel activation and a
30 431 consequent K^+ efflux) and net H^+ effluxes were similar between PNC-inoculated and NNP-
31 432 inoculated leaves under salt stress (Fig. 5C, 5D, and 7A). Together, our pharmacological studies
32 433 indicate that ROS-NSCC but not GORK channels are major contributors to the $\cdot OH$ induced K^+
33 434 efflux in mesophyll cells. Improved K^+ retention is mainly achieved by PNC scavenging of $\cdot OH$
34 435 but not H_2O_2 or superoxide anion. As it has been reported in roots,³⁴ $\cdot OH$ exerts the strongest
35 436 modulation of the activities of ROS-activated NSCC and GORK channels in leaves (Fig. 6). To
36 437 assess the impact of nanoceria ROS scavenging on the contribution of ATP dependent K^+/H^+
37 438 symporters e.g., HAK5 in mesophyll K^+ retention, we measured whole leaf ATP content.
38
39
40
41
42
43
44
45
46
47
48
49
50
51
52
53
54
55
56
57
58
59
60

1
2
3 439 However, we found no differences in ATP levels between PNC- and NNP-inoculated leaves
4 440 under salt stress (Fig. 7B).

5
6 441
7
8 442 ROS accumulation is a well-known secondary stress accompanying salt stress in plants.⁷⁰ PNC
9 443 reduces accumulation of ROS in plants under salt stress including $\cdot\text{OH}$ that cannot be scavenged
10 444 by any known enzymes (Fig. 3A, 3C, and 3D, Fig. 6). Cerium oxide nanoparticles have been
11 445 reported to scavenge $\cdot\text{OH}$ *in vitro*.¹³ In this study, *Arabidopsis* PNC-Leaves have 41 % lower
12 446 HPF intensity, an indicator of $\cdot\text{OH}$, than control NNP-leaves under salinity stress. PNC-Leaves
13 447 also have 48 % lower $\cdot\text{OH}$ -induced K^+ efflux than NNP-Leaves (Fig. 6A). ROS homeostasis is
14 448 crucial for maintaining K^+ mesophyll retention, a key trait for plant salt tolerance.^{30–32,72} In plant
15 449 root cells under salt stress, $\cdot\text{OH}$ is known to activate GORK and NSCC channels leading to
16 450 increased K^+ efflux in plants root cells.^{33,34,73} Here we report that $\cdot\text{OH}$ induced leaf mesophyll K^+
17 451 efflux is over 10 times higher than that generated by H_2O_2 (Fig. 6). The K^+ efflux induced by
18 452 H_2O_2 might be due to conversion of H_2O_2 to $\cdot\text{OH}$ by cell-wall transition metals and
19 453 ascorbate.^{74,75} We assessed the direct impact of $\cdot\text{OH}$ on mesophyll K^+ retention and whether
20 454 ROS-NSCC or GORK channels play a main role in controlling $\cdot\text{OH}$ -induced K^+ efflux. Our
21 455 results indicate that $\cdot\text{OH}$ can induce a significant K^+ efflux in *Arabidopsis* leaf mesophyll, and
22 456 ROS-activated NSCC channels but not GORK channel play a major role in this process (Fig. 6,
23 457 Fig. 7). Besides its role in elongation/expansion of plant cells,^{35,76} ROS-activated NSCC
24 458 channels are known to be involved in NaCl-induced K^+ efflux in root⁷⁷ and mesophyll⁷⁸ cells.
25 459 Overall, our results indicate that PNC augmented $\cdot\text{OH}$ scavenging modulates activities of ROS-
26 460 activated NSCC and GORK channels and reduces K^+ loss from cytosol, thus improving plant
27 461 salinity stress tolerance.

28
29
30
31
32
33
34
35
36
37
38
39
40
41
42
43
44
45
46
47
48
49
50
51
52
53
54
55
56
57
58
59
60

3.4. Nanoceria effect on K^+ channel and transporter transcription levels in leaves

46 464 To further understand the effect of nanoceria on K^+ mesophyll transport in leaves of *Arabidopsis*
47 465 plants under salt stress, we assessed the relative gene expression of a set of channels/transporters
48 466 involved in K^+ transport. No significant changes in relative gene expression of *gork* were found
49 467 between PNC-leaves and NNP-leaves under salt stress (Fig. 7C). The K^+ influx symporter *HAK5*
50 468 gene was significantly upregulated in PNC-leaves (Fig. 7C). HAK/KUP is a family of
51 469 symporters that are key in K^+ uptake of plants under salt stress. Although *HAK5* gene encoding

1
2
3 470 K^+/H^+ symporter was upregulated, its co-transport activity is dependent on the H^+
4
5 471 electrochemical gradient across plasma membrane that requires ATP. The generation of ATP is
6
7 472 well known to be reduced in plants under salt stress.^{79,80} We recorded a 50 % drop of ATP
8
9 473 content in leaves under salt stress (Fig. 7B) but no differences in the ATP content between PNC-
10
11 474 and NNP- inoculated leaves. Thus, HAK5 active transporter contribution to K^+ retention is not
12
13 475 expected to be significant compared to NSCC and GORK channels due to low ATP levels (Fig.
14
15 476 7B). Relative gene expression of H^+ -ATPase (Fig. 7C) and net H^+ efflux (Fig. 5C and 5D) in
16
17 477 PNC-leaves were similar to NNP-leaves under salt stress. H^+ -ATPase pumps H^+ from the cell
18
19 478 cytosol to the extra cellular space (apoplast), building up the electrochemical gradient that forms
20
21 479 the plasma membrane potential.⁶⁶ Plasma membrane depolarization occurs immediately after
22
23 480 onset of salt stress in plants.⁶⁸ Here we found that the degree of plasma membrane potential
24
25 481 depolarization in PNC-leaves was also similar to NNP-leaves (Fig. 7A). Thus improved
26
27 482 mesophyll K^+ retention was unlikely due to lower depolarization of the plasma membrane
28
29 483 potential enabled by PNC ROS scavenging under salt stress. The *NHX1* gene (a tonoplast K^+ ,
30
31 484 Na^+/H^+ antiporter) was upregulated whereas the relative expression of *Avp* gene (a tonoplast
32
33 485 PPase-driven hydrogen pump which fuels the *NHX1* antiporter)⁸¹ was downregulated in PNC-
34
35 486 leaves relative to NNP-leaves under salt stress (Fig. 7C). Therefore the import of K^+ through
36
37 487 *NHX1* from cytosol to vacuole⁸² might be compromised by the lower H^+ electrochemical
38
39 488 gradient provided by H^+ -PPase. In accordance with these results, no significant differences were
40
41 489 found in the vacuole APG-2 (K^+ dye) intensity between PNC-leaves and NNP-leaves under high
42
43 490 salinity (Fig. 4B). Relative expression of proton pump *Aha* gene was not significantly different
44
45 491 between PNC- and NNP-inoculated leaves under salt stress (Fig. 7C).

46
47
48
49
50
51
52
53
54
55
56
57
58
59
60

4. Conclusion

493
494 Maintaining plant cell K^+ retention is regarded as a mechanism to improve salinity stress
495 tolerance in crops.⁸³ In this study, we show that PNC scavenging of $\cdot OH$ and its precursors leads
496 to higher leaf mesophyll K^+ retention under salinity stress. PNC increase photosynthetic carbon
497 assimilation rates and quantum yield of PSII, and shoot biomass in *Arabidopsis* under salinity
498 stress. PNC ability to localize inside plant cells and catalytically reducing $\cdot OH$ (Fig. 3) is a key
499 tool for understanding the role of ROS in plant stress responses and elucidate plant-nanoceria
500 interactions. Like hydrogen peroxide, $\cdot OH$ has been proposed to have a dual role in plant

1
2
3 501 physiology acting as harmful molecules at high levels and being involved in stress signaling at
4 502 low concentration.^{84,85,86,87} However, current chemical based tools for *in vivo* $\cdot\text{OH}$
5 503 scavenging^{88,89,90} cannot sustain long term catalytic scavenging as nanoceria. Herein, we show
6 504 that PNC catalytic scavenging of $\cdot\text{OH}$ strongly influences the activity of ROS-NSCC and GORK
7 505 channels in plant leaves, key plasma membrane channels controlling plant cell K^+ retention. To
8 506 meet the food demand for the projected 9.3 billion human population at 2050, agricultural
9 507 production needs to be increased by 60 % from the 2005-2007 level.⁹¹ Land salinization is a
10 508 main limitation for agricultural production worldwide⁹² that is being exacerbated by a changing
11 509 climate⁹³ and utilization of fertilizers⁹⁴ resulting in multi-billion dollar annual losses⁹⁵. Scalable
12 510 and economical foliar spray delivery methods of PNC may alleviate oxidative stress and
13 511 mesophyll K^+ loss caused by salt stress and improve crop growth and yield.
14
15
16
17
18
19
20
21
22
23

24 513 **Conflict of interest**

25 514 The authors declare no competing financial interest.
26
27
28

29 516 **Acknowledgements**

30 517 This material is based upon work supported by the National Science Foundation under Grant No.
31 518 1817363 to J.P.G. This work was supported by the University of California, Riverside and
32 519 USDA National Institute of Food and Agriculture, Hatch project 1009710 to J.P.G and ARC and
33 520 GRDC grants to S.S.
34
35
36
37
38

39 522 **References**

- 40
41 523 1 A. Fita, A. Rodríguez-Burruezo, M. Boscaiu, J. Prohens and O. Vicente, *Breeding and*
42 524 *domesticating crops adapted to drought and salinity: A new paradigm for increasing food*
43 525 *production, Front. Plant Sci.*, 2015, **6**, 978.
44
45 526 2 R. Munns and M. Tester, *Mechanisms of salinity tolerance, Annu. Rev. Plant Biol.*, 2008,
46 527 **59**, 651–681.
47
48 528 3 V. Demidchik, *Mechanisms of oxidative stress in plants: From classical chemistry to cell*
49 529 *biology, Environ. Exp. Bot.*, 2015, **109**, 212–228.
50
51 530 4 S. S. Gill and N. Tuteja, *Reactive oxygen species and antioxidant machinery in abiotic*
52 531 *stress tolerance in crop plants, Plant Physiol. Biochem.*, 2010, **48**, 909–930.
53
54
55
56
57
58
59
60

- 1
2
3 532 5 Y. G. Song, B. Liu, L. F. Wang, M. H. Li and Y. Liu, *Damage to the oxygen-evolving*
4 533 *complex by superoxide anion, hydrogen peroxide, and hydroxyl radical in photoinhibition*
5 534 *of photosystem II, Photosynth. Res.*, 2006, **90**, 67–78.
- 6
7
8 535 6 H. Sies, *Strategies of antioxidant defense, Eur. J. Biochem.*, 1993, **215**, 213–219.
- 9
10 536 7 K. Das and A. Roychoudhury, *Reactive oxygen species (ROS) and response of*
11 537 *antioxidants as ROS-scavengers during environmental stress in plants, Front. Environ.*
12 538 *Sci.*, 2014, **2**, 1–13.
- 13
14
15 539 8 J. P. Giraldo, M. P. Landry, S. M. Faltermeier, T. P. McNicholas, N. M. Iverson, A. A.
16 540 Boghossian, N. F. Reuel, A. J. Hilmer, F. Sen, J. A. Brew and M. S. Strano, *Plant*
17 541 *nanobionics approach to augment photosynthesis and biochemical sensing, Nat. Mater.*,
18 542 2014, **13**, 400–408.
- 19
20
21
22 543 9 W. Du, W. Tan, J. R. Peralta-Videoa, J. L. Gardea-Torresdey, R. Ji, Y. Yin and H. Guo,
23 544 *Interaction of metal oxide nanoparticles with higher terrestrial plants: Physiological and*
24 545 *biochemical aspects, Plant Physiol. Biochem.*, 2017, **110**, 210–225.
- 25
26
27 546 10 A. Pérez-de-Luque, *Interaction of nanomaterials with plants: What do we need for real*
28 547 *applications in agriculture?, Front. Environ. Sci.*, 2017, **5**, 1–7.
- 29
30
31 548 11 P. Wang, E. Lombi, F. J. Zhao and P. M. Kopittke, *Nanotechnology: A new opportunity in*
32 549 *plant sciences, Trends Plant Sci.*, 2016, **21**, 699–712.
- 33
34 550 12 M. H. Wong, J. P. Giraldo, S. Y. Kwak, V. B. Koman, R. Sinclair, T. T. S. Lew, G. Bisker,
35 551 P. Liu and M. S. Strano, *Nitroaromatic detection and infrared communication from wild-*
36 552 *type plants using plant nanobionics.*, *Nat. Mater.*, 2017, **16**, 264–272.
- 37
38
39 553 13 Y. Xue, Q. Luan, D. Yang, X. Yao and K. Zhou, *Direct evidence for hydroxyl radical*
40 554 *scavenging activity of cerium oxide nanoparticles, J. Phys. Chem. C*, 2011, **115**, 4433–
41 555 4438.
- 42
43
44 556 14 B. Nelson, M. Johnson, M. Walker, K. Riley and C. Sims, *Antioxidant cerium oxide*
45 557 *nanoparticles in biology and medicine, Antioxidants*, 2016, **5**, 15.
- 46
47
48 558 15 C. Walkey, S. Das, S. Seal, J. Erlichman, K. Heckman, L. Ghibelli, E. Traversa, J. F.
49 559 McGinnis and W. T. Self, *Catalytic properties and biomedical applications of cerium*
50 560 *oxide nanoparticles, Environ. Sci. Nano*, 2015, **2**, 33–53.
- 51
52
53 561 16 G. Pulido-Reyes, I. Rodea-Palomares, S. Das, T. S. Sakthivel, F. Leganes, R. Rosal, S.
54 562 Seal and F. Fernández-Piñas, *Untangling the biological effects of cerium oxide*

- 1
2
3 563 *nanoparticles: the role of surface valence states*, *Sci. Rep.*, 2015, **5**, 15613.
- 4
5 564 17 P. Dutta, S. Pal, M. S. Seehra, Y. Shi, E. M. Eyring and R. D. Ernst, *Concentration of*
6 565 *Ce³⁺ and oxygen vacancies in cerium oxide nanoparticles*, *Chem. Mater.*, 2006, **18**, 5144–
7 566 5146.
- 8
9
10 567 18 A. A. Boghossian, F. Sen, B. M. Gibbons, S. Sen, S. M. Faltermeier, J. P. Giraldo, C. T.
11 568 Zhang, J. Zhang and M. S. Strano, *Application of nanoparticle antioxidants to enable*
12 569 *hyperstable chloroplasts for solar energy harvesting*, *Adv. Energy Mater.*, 2013, **3**, 881–
13 570 893.
- 14
15
16
17 571 19 H. Wu, N. Tito and J. P. Giraldo, *Anionic cerium oxide nanoparticles protect plant*
18 572 *photosynthesis from abiotic stress by scavenging reactive oxygen species*, *ACS Nano*,
19 573 2017, **11**, 11283–11297.
- 20
21
22 574 20 S. D. Ebbs, S. J. Bradfield, P. Kumar, J. C. White, C. Musante and X. Ma, *Accumulation*
23 575 *of zinc, copper, or cerium in carrot (Daucus carota) exposed to metal oxide nanoparticles*
24 576 *and metal ions*, *Environ. Sci. Nano*, 2016, **3**, 114–126.
- 25
26
27 577 21 C. M. Rico, M. G. Johnson, M. A. Marcus and C. P. Andersen, *Intergenerational*
28 578 *responses of wheat (Triticum aestivum L.) to cerium oxide nanoparticles exposure*,
29 579 *Environ. Sci. Nano*, 2017, **4**, 700–711.
- 30
31
32 580 22 E. Spielman-Sun, E. Lombi, E. Donner, D. Howard, J. M. Unrine and G. V. Lowry,
33 581 *Impact of surface charge on cerium oxide nanoparticle uptake and translocation by wheat*
34 582 *(Triticum aestivum)*, *Environ. Sci. Technol.*, 2017, **51**, 7361–7368.
- 35
36
37 583 23 L. Pagano, F. Pasquali, S. Majumdar, R. De la Torre-Roche, N. Zuverza-Mena, M. Villani,
38 584 A. Zappettini, R. E. Marra, S. M. Isch, M. Marmioli, E. Maestri, O. P. Dhankher, J. C.
39 585 White and N. Marmioli, *Exposure of Cucurbita pepo to binary combinations of*
40 586 *engineered nanomaterials: physiological and molecular response*, *Environ. Sci. Nano*,
41 587 2017, **4**, 1579–1590.
- 42
43
44
45
46 588 24 L. Rossi, H. Sharifan, W. Zhang, A. P. Schwab and X. Ma, *Mutual effects and in-planta*
47 589 *accumulation of co-existing cerium oxide nanoparticles and cadmium in hydroponically*
48 590 *grown soybean (Glycine max (L.) Merr.)*, *Environmental Sci. Nano*, 2018, **5**, 150–157.
- 49
50
51 591 25 C. Ma, H. Liu, H. Guo, C. Musante, S. H. Coskun, B. C. Nelson, J. C. White, B. Xing and
52 592 O. P. Dhankher, *Defense mechanisms and nutrient displacement in Arabidopsis thaliana*
53 593 *upon exposure to CeO₂ and In₂O₃ nanoparticles*, *Environ. Sci. Nano*, 2016, **3**, 1369–1379.
- 54
55
56
57
58
59
60

- 1
2
3 594 26 D. Cui, P. Zhang, Y. Ma, X. He, Y. Li, J. Zhang, Y. Zhao and Z. Zhang, *Effect of cerium*
4 *oxide nanoparticles on asparagus lettuce cultured in an agar medium*, *Environ. Sci. Nano*,
5 595 2014, **1**, 459–465.
6
7 596
8 597 27 L. Rossi, W. Zhang, L. Lombardini and X. Ma, *The impact of cerium oxide nanoparticles*
9 *on the salt stress responses of Brassica napus L.*, *Environ. Pollut.*, 2016, **219**, 28–36.
10 598
11 599 28 Z. Cao, C. Stowers, L. Rossi, W. Zhang, L. Lombardini and X. Ma, *Physiological effects*
12 *of cerium oxide nanoparticles on the photosynthesis and water use efficiency of soybean*
13 *(Glycine max (L.) Merr.)*, *Environ. Sci. Nano*, 2017, **4**, 1086–1094.
14 600
15 601
16 602 29 I. Hussain, N. B. Singh, A. Singh, H. Singh, S. C. Singh and V. Yadav, *Exogenous*
17 *application of phytosynthesized nanoceria to alleviate ferulic acid stress in Solanum*
18 *lycopersicum*, *Sci. Hortic. (Amsterdam)*, 2017, **214**, 158–164.
19 603
20 604
21 605 30 H. Wu, L. Shabala, M. Zhou and S. Shabala, *Durum and bread wheat differ in their ability*
22 *to retain potassium in leaf mesophyll: Implications for salinity stress tolerance*, *Plant Cell*
23 *Physiol.*, 2014, **55**, 1749–1762.
24 606
25 607
26 608 31 H. Wu, M. Zhu, L. Shabala, M. Zhou and S. Shabala, *K⁺ retention in leaf mesophyll, an*
27 *overlooked component of salinity tolerance mechanism: A case study for barley*, *J. Integr.*
28 *Plant Biol.*, 2015, **57**, 171–185.
29 609
30 610
31 611 32 H. Wu, L. Shabala, K. Barry, M. Zhou and S. Shabala, *Ability of leaf mesophyll to retain*
32 *potassium correlates with salinity tolerance in wheat and barley*, *Physiol. Plant.*, 2013,
33 612 **149**, 515–527.
34 613
35 614 33 V. Demidchik and F. J. M. Maathuis, *Physiological roles of nonselective cation channels*
36 *in plants: from salt stress to signalling and development*, *New Phytol.*, 2007, **175**, 387–
37 615 404.
38 616
39 617 34 V. Demidchik, T. A. Cuin, D. Svistunenko, S. J. Smith, A. J. Miller, S. Shabala, A.
40 *Sokolik and V. Yurin, Arabidopsis root K⁺-efflux conductance activated by hydroxyl*
41 *radicals: single-channel properties, genetic basis and involvement in stress-induced cell*
42 *death*, *J. Cell Sci.*, 2010, **123**, 1468–1479.
43 618
44 619
45 620 35 V. Demidchik, S. N. Shabala, K. B. Coutts, M. A. Tester and J. M. Davies, *Free oxygen*
46 *radicals regulate plasma membrane Ca²⁺- and K⁺-permeable channels in plant root cells.*,
47 *J. Cell Sci.*, 2003, **116**, 81–88.
48 621
49 622
50 623
51 624 36 I. Zepeda-Jazo, A. M. Velarde-Buendia, R. Enriquez-Figueroa, J. Bose, S. Shabala, J.

- 1
2
3 625 Muniz-Murguia and I. I. Pottosin, *Polyamines interact with hydroxyl radicals in activating*
4 626 *Ca²⁺ and K⁺ transport across the root epidermal plasma membranes*, *Plant Physiol.*, 2011,
5 627 **157**, 2167–2180.
- 6
7
8 628 37 M. Safi, H. Sarrouj, O. Sandre, N. Mignet and J. F. Berret, *Interactions between sub-10-*
9 629 *nm iron and cerium oxide nanoparticles and 3T3 fibroblasts: the role of the coating and*
10 630 *aggregation state*, *Nanotechnology*, 2010, **21**, 145103.
- 11
12
13 631 38 H. Wu, I. Santana, J. Dansie and J. P. Giraldo, *In vivo delivery of nanoparticles into plant*
14 632 *leaves.*, *Curr. Protoc. Chem. Biol.*, 2017, **9**, 269–284.
- 15
16
17 633 39 H. Shi, H. Shi, L. Xiong, L. Xiong, B. Stevenson, B. Stevenson, T. Lu, T. Lu, J. Zhu and J.
18 634 *Zhu*, *The Arabidopsis salt overly sensitive 4 mutants uncover a critical role for vitamin B6*
19 635 *in plant salt tolerance*, *Plant Cell*, 2002, **14**, 575–588.
- 20
21
22 636 40 H. Shi, M. Ishitani, C. Kim and J.K. Zhu, *The Arabidopsis thaliana salt tolerance gene*
23 637 *SOS1 encodes a putative Na⁺/H⁺ antiporter*, *Proc. Natl. Acad. Sci.*, 2000, **97**, 6896–6901.
- 24
25
26 638 41 J. Bose, Y. Xie, W. Shen and S. Shabala, *Haem oxygenase modifies salinity tolerance in*
27 639 *Arabidopsis by controlling K⁺ retention via regulation of the plasma membrane H⁺-*
28 640 *ATPase and by altering SOS1 transcript levels in roots*, *J. Exp. Bot.*, 2013, **64**, 471–481.
- 29
30
31 641 42 D. Kumar, M. A. Yusuf, P. Singh, M. Sardar and N. B. Sarin, *Modulation of antioxidant*
32 642 *machinery in α-tocopherol-enriched transgenic Brassica juncea plants tolerant to abiotic*
33 643 *stress conditions*, *Protoplasma*, 2013, **250**, 1079–1089.
- 34
35
36 644 43 S. Shabala, V. Demidchik, L. Shabala, T. A. Cuin, S. J. Smith, A. J. Miller, J. M. Davies
37 645 and I. A. Newman, *Extracellular Ca²⁺ ameliorates NaCl-induced K⁺ loss from*
38 646 *Arabidopsis root and leaf cells by controlling plasma membrane K⁺-permeable channels*,
39 647 *Plant Physiol.*, 2006, **141**, 1653–1665.
- 40
41
42
43 648 44 I. A. Newman, *Ion transport in roots: measurement of fluxes using ion-selective*
44 649 *microelectrodes to characterize transporter function*, *Plant. Cell Environ.*, 2001, **24**, 1–14.
- 45
46
47 650 45 F. Zeng, L. Shabala, M. Zhou, G. Zhang and S. Shabala, *Barley responses to combined*
48 651 *waterlogging and salinity stress: separating effects of oxygen deprivation and elemental*
49 652 *toxicity*, *Front. Plant Sci.*, 2013, **4**, 1–13.
- 50
51
52 653 46 D. F. Gaff and H. Ziegler, *ATP and ADP contents in leaves of drying and rehydrating*
53 654 *desiccation tolerant plants*, *Oecologia*, 1989, **78**, 407–410.
- 54
55 655 47 G. Brychkova, Z. Xia, G. Yang, Z. Yesbergenova, Z. Zhang, O. Davydov, R. Fluhr and M.

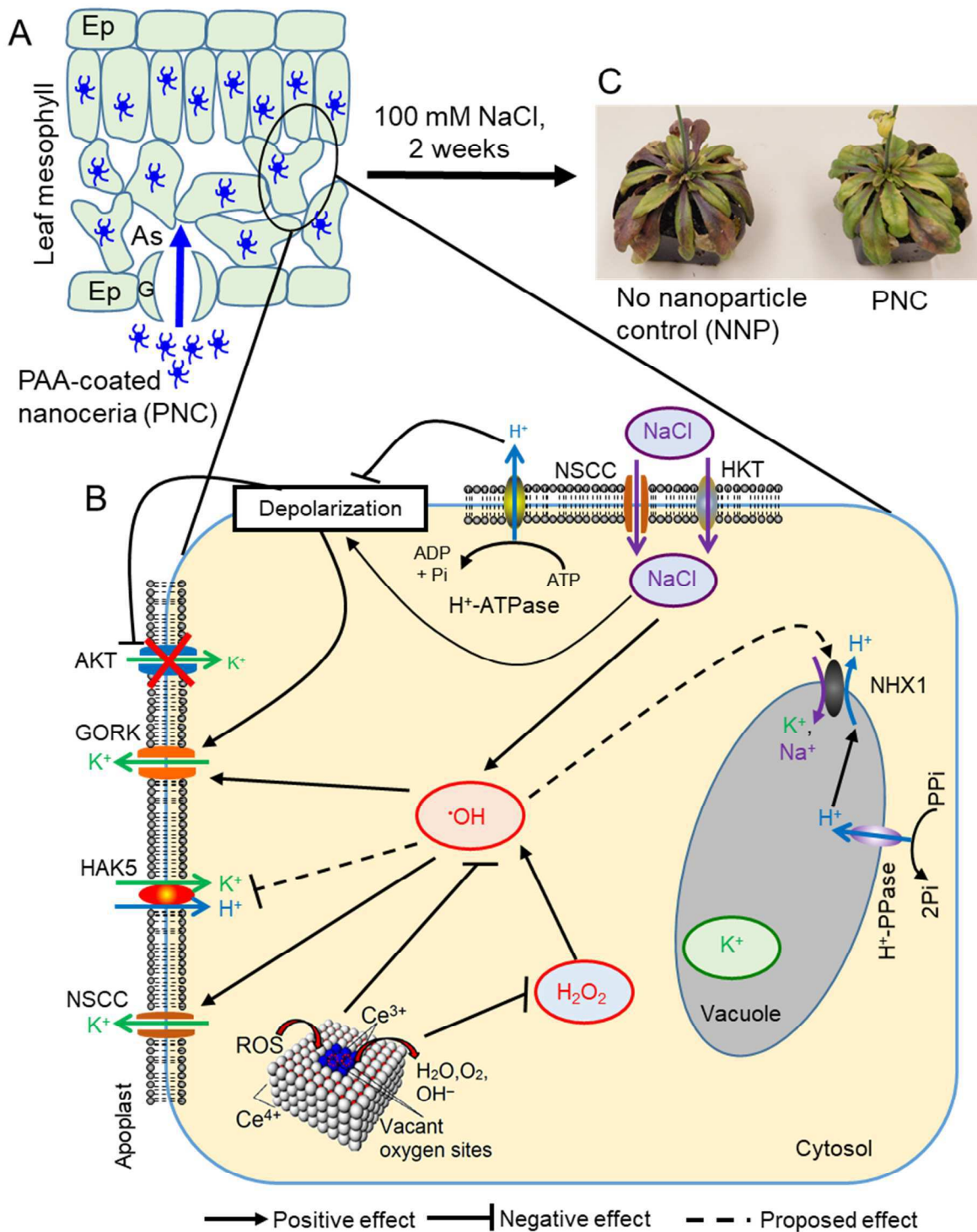
- 1
2
3 656 Sagi, *Sulfite oxidase protects plants against sulfur dioxide toxicity*, *Plant J.*, 2007, **50**,
4 657 696–709.
- 6 658 48 J. Vandesompele, K. De Preter, F. Pattyn, B. Poppe, N. Van Roy, A. De Paepe and F.
8 659 Speleman, *Accurate normalization of real-time quantitative RT-PCR data by geometric*
9 660 *averaging of multiple internal control genes*, *Genome Biol.*, 2002, **3**, research0034.1-
11 661 research0034.11.
- 13 662 49 K. J. Livak and T. D. Schmittgen, *Analysis of relative gene expression data using real-*
15 663 *time quantitative PCR and the $2^{-\Delta\Delta CT}$ method*, *Methods*, 2001, **25**, 402–408.
- 17 664 50 Y. Xie, Y. Mao, W. Zhang, D. Lai, Q. Wang and W. Shen, *Reactive oxygen species-*
18 665 *dependent nitric oxide production contributes to hydrogen-promoted stomatal closure in*
20 666 *Arabidopsis*, *Plant Physiol.*, 2014, **165**, 759–773.
- 22 667 51 M. Nieves-Cordones, F. Alemán, V. Martínez and F. Rubio, *The Arabidopsis thaliana*
23 668 *HAK5 K^+ transporter is required for plant growth and K^+ acquisition from low K^+*
25 669 *solutions under saline conditions*, *Mol. Plant*, 2010, **3**, 326–333.
- 27 670 52 D. H. Oh, S. Y. Lee, R. A. Bressan, D. J. Yun and H. J. Bohnert, *Intracellular*
28 671 *consequences of SOS1 deficiency during salt stress*, *J. Exp. Bot.*, 2010, **61**, 1205–1213.
- 30 672 53 R. A. Volkov, I. I. Panchuk and F. Schöffl, *Heat-stress-dependency and developmental*
32 673 *modulation of gene expression: The potential of house-keeping genes as internal*
34 674 *standards in mRNA expression profiling using real-time RT-PCR*, *J. Exp. Bot.*, 2003, **54**,
35 675 2343–2349.
- 37 676 54 S. J. Coon, M. Gilliam, A. Athman, A. W. Schreiber, T. Baumann, I. Moller, N. H.
39 677 Cheng, M. A. Stancombe, K. D. Hirschi, A. A. R. Webb, R. Burton, B. N. Kaiser, S. D.
41 678 Tyerman and R. A. Leigh, *Cell-specific vacuolar calcium storage mediated by CAX1*
42 679 *regulates apoplastic calcium concentration, gas exchange, and plant productivity in*
44 680 *Arabidopsis*, *Plant Cell*, 2011, **23**, 240–257.
- 46 681 55 W. W. Zhang, J. J. Meng, J. Y. Xing, S. Yang, F. Guo, X. G. Li and S. B. Wan, *The*
47 682 *K^+/H^+ antiporter AhNHX1 improved tobacco tolerance to NaCl stress by enhancing K^+*
49 683 *retention*, *J. Plant Biol.*, 2017, **60**, 259–267.
- 51 684 56 W. Zhang, S. D. Ebbs, C. Musante, J. C. White, C. Gao and X. Ma, *Uptake and*
52 685 *accumulation of bulk and nanosized cerium oxide particles and ionic cerium by radish*
54 686 *(Raphanus sativus L.)*, *J. Agric. Food Chem.*, 2015, **63**, 382–390.

- 1
2
3 687 57 K. Setsukinai, Y. Urano, K. Kakinuma, H. J. Majima and T. Nagano, *Development of*
4 688 *novel fluorescence probes that can reliably detect reactive oxygen species and distinguish*
5 689 *specific species, J. Biol. Chem.*, 2003, **278**, 3170–3175.
- 6
7
8 690 58 M. Price, J. J. Reiners, A. M. Santiago and D. Kessel, *Monitoring singlet oxygen and*
9 691 *hydroxyl radical formation with fluorescent probes during photodynamic therapy,*
10 692 *Photochem. Photobiol.*, 2009, **85**, 1177–1181.
- 11
12
13 693 59 H. Zhao, J. Joseph, H. M. Fales, E. A. Sokoloski, R. L. Levine, J. Vasquez-Vivar and B.
14 694 Kalyanaraman, *Detection and characterization of the product of hydroethidine and*
15 695 *intracellular superoxide by HPLC and limitations of fluorescence, Proc. Natl. Acad. Sci.*,
16 696 2005, **102**, 5727–5732.
- 17
18
19 697 60 V. Demidchik, *ROS-activated ion channels in plants: Biophysical characteristics,*
20 698 *physiological functions and molecular nature, Int. J. Mol. Sci.*, 2018, **19**, 1263.
- 21
22
23 699 61 S. Shabala, *Signalling by potassium: Another second messenger to add to the list?, J. Exp.*
24 700 *Bot.*, 2017, **68**, 4003–4007.
- 25
26
27 701 62 L. Shabala, J. Zhang, I. Pottosin, J. Bose, M. Zhu, A. T. Fuglsang, A. Velarde-Buendia, A.
28 702 Massart, C. B. Hill, U. Roessner, A. Bacic, H. Wu, E. Azzarello, C. Pandolfi, M. Zhou, C.
29 703 Poschenrieder, S. Mancuso and S. Shabala, *Cell-type-specific H⁺-ATPase activity in root*
30 704 *tissues enables K⁺ retention and mediates acclimation of barley (*Hordeum vulgare*) to*
31 705 *salinity stress, Plant Physiol.*, 2016, **172**, 2445–2458.
- 32
33
34 706 63 P. C. Sijmons, F. C. Lanfermeijer, A. H. de Boer, H. B. Prins and H. F. Bienfait,
35 707 *Depolarization of cell membrane potential during trans-plasma membrane electron*
36 708 *transfer to extracellular electron acceptors in iron-deficient roots of *Phaseolus vulgaris* L.,*
37 709 *Plant Physiol.*, 2014, **76**, 943–946.
- 38
39
40 710 64 C. I. Ullrich and A. J. Novacky, *Extra- and intracellular pH and membrane potential*
41 711 *changes induced by K⁺, Cl⁻, H₂PO₄⁻, and NO₃⁻ uptake and fusicoccin in root hairs of*
42 712 **Limnobium stoloniferum*, Plant Physiol.*, 1990, **94**, 1561–1567.
- 43
44
45 713 65 A. Conde, M. M. Chaves and H. Gerós, *Membrane transport, sensing and signaling in*
46 714 *plant adaptation to environmental stress, Plant Cell Physiol.*, 2011, **52**, 1583–1602.
- 47
48
49 715 66 M. G. Palmgren, *Plant plasma membrane H⁺-ATPases, Annu. Rev. Plant Biol.*, 2001, **52**,
50 716 817–845.
- 51
52
53 717 67 Z. Chen, I. I. Pottosin, T. A. Cuin, A. T. Fuglsang, M. Tester, D. Jha, I. Zepeda-jazo, M.

- 1
2
3 718 Zhou, M. G. Palmgren, I. A. Newman and S. Shabala, *Root plasma membrane*
4 *transporters controlling K^+/Na^+ homeostasis in salt-stressed barley*, *Plant Physiol.*, 2007,
5 719 **145**, 1714–1725.
6
7 720
8
9 721 68 L. Shabala, T. A. Cuin, I. A. Newman and S. Shabala, *Salinity-induced ion flux patterns*
10 722 *from the excised roots of Arabidopsis sos mutants*, *Planta*, 2005, **222**, 1041–1050.
11
12 723 69 A. Sosan, D. Svistunenko, D. Straltsova, K. Tsiurkina, I. Smolich, T. Lawson, S.
13 724 Subramaniam, V. Golovko, D. Anderson, A. Sokolik, I. Colbeck and V. Demidchik,
14 *Engineered silver nanoparticles are sensed at the plasma membrane and dramatically*
15 725 *modify the physiology of Arabidopsis thaliana plants*, *Plant J.*, 2016, **85**, 245–257.
16 726
17 727 70 J. K. Zhu, *Abiotic stress signaling and responses in plants*, *Cell*, 2016, **167**, 313–324.
18
19 728 71 T. A. Cuin and S. Shabala, *Compatible solutes reduce ROS-induced potassium efflux in*
20 *Arabidopsis roots*, *Plant, Cell Environ.*, 2007, **30**, 875–885.
21 729
22 730 72 J. You and Z. Chan, *ROS regulation during abiotic stress responses in crop plants*, *Front.*
23 *Plant Sci.*, 2015, **6**, 1092.
24 731
25 732 73 G. Adem, S. J. Roy, M. Zhou, J. P. Bowman and S. Shabala, *Evaluating contribution of*
26 *ionic, osmotic and oxidative stress components towards salinity tolerance in barley*, *BMC*
27 *Plant Biol.*, 2014, **14**, 113.
28 733
29 734 74 S. C. Fry, J. G. Miller and J. C. Dumville, *A proposed role for copper ions in cell wall*
30 *loosening*, *Plant Soil*, 2002, **247**, 57–67.
31 735
32 736 75 S. C. Fry, *Primary cell wall: tracking the careers of wall polymers in living plant cells*,
33 *New Phytol.*, 2004, **161**, 641–675.
34 737
35 738 76 J. Foreman, V. Demidchik, J. H. F. Bothwell, P. Mylona, H. Miedema, M. A. Torres, P.
36 739 Linstead, S. Costa, C. Brownlee, J. D. G. Jones, J. M. Davies and L. Dolan, *Reactive*
37 *oxygen species produced by NADPH oxidase regulate plant cell growth*, *Nature*, 2003,
38 740 **422**, 442–446.
39 741
40 742
41 743 77 M. Jayakannan, J. Bose, O. Babourina, Z. Rengel and S. Shabala, *Salicylic acid improves*
42 *salinity tolerance in Arabidopsis by restoring membrane potential and preventing salt-*
43 *induced K^+ loss via a GORK channel*, *J. Exp. Bot.*, 2013, **64**, 2255–2268.
44 744
45 745
46 746 78 H. Wu, L. Shabala, M. Zhou and S. Shabala, *Chloroplast-generated ROS dominate NaCl-*
47 *induced K^+ efflux in wheat leaf mesophyll*, *Plant Signal. Behav.*, 2015, **10**, e1013793.
48 747
49 748 79 J. Bose, L. Shabala, I. Pottosin, F. Zeng, A. Velarde-Buendie, A. Massart, C.
50
51
52
53
54
55
56
57
58
59
60

- 1
2
3 749 Poschenrieder, Y. Hariadi and S. Shabala, *Kinetics of xylem loading, membrane potential*
4 *maintenance, and sensitivity of K^+ -permeable channels to reactive oxygen species:*
5 750 *physiological traits that differentiate salinity tolerance between pea and barley, Plant.*
6 *Cell Environ.*, 2014, **37**, 589–600.
7 751
8 752
9
10 753 80 X. Ma, L. Deng, J. Li, X. Zhou, N. Li, D. Zhang, Y. Lu, R. Wang, J. Sun, C. Lu, X. Zheng,
11 *E. Fritz, A. Hüttermann and S. Chen, Effect of NaCl on leaf H^+ -ATPase and the relevance*
12 754 *to salt tolerance in two contrasting poplar species, Trees*, 2010, **24**, 597–607.
13 755
14
15 756 81 P. Silva and H. Gerós, *Regulation by salt of vacuolar H^+ -ATPase and H^+ -*
16 *pyrophosphatase activities and Na^+/H^+ exchange, Plant Signal. Behav.*, 2009, **4**, 718–726.
17 757
18
19 758 82 E. Bassil, H. Tajima, Y. C. Liang, M. A. Ohto, K. Ushijima, R. Nakano, T. Esumi, A.
20 *Coku, M. Belmonte and E. Blumwald, The Arabidopsis Na^+/H^+ antiporters NHX1 and*
21 759 *NHX2 control vacuolar pH and K^+ homeostasis to regulate growth, flower development,*
22 760 *and reproduction, Plant Cell*, 2011, **23**, 3482–3497.
23 761
24
25 762 83 A. M. Ismail and T. Horie, *Genomics, physiology, and molecular breeding approaches for*
26 *improving salt tolerance, Annu. Rev. Plant Biol.*, 2017, **68**, 405–434.
27 763
28
29 764 84 S. L. Richards, K. A. Wilkins, S. M. Swarbreck, A. A. Anderson, N. Habib, A. G. Smith,
30 *M. McAinsh and J. M. Davies, The hydroxyl radical in plants: from seed to seed, J. Exp.*
31 765 *Bot.*, 2015, **66**, 37–46.
32 766
33
34 767 85 P. Schopfer, *Hydroxyl radical-induced cell-wall loosening in vitro and in vivo:*
35 *Implications for the control of elongation growth, Plant J.*, 2001, **28**, 679–688.
36 768
37
38 769 86 K. Muller, A. Linkies, R. A. M. Vreeburg, S. C. Fry, A. Krieger-Liszkay and G. Leubner-
39 *Metzger, In vivo cell wall loosening by hydroxyl radicals during cress seed germination*
40 770 *and elongation growth, Plant Physiol.*, 2009, **150**, 1855–1865.
41 771
42
43 772 87 L. H. Hao, W. X. Wang, C. Chen, Y. F. Wang, T. Liu, X. Li and Z. L. Shang,
44 *Extracellular ATP promotes stomatal opening of Arabidopsis thaliana through*
45 773 *heterotrimeric G protein α subunit and reactive oxygen species, Mol. Plant*, 2012, **5**, 852–
46 774 864.
47
48 775
49
50 776 88 S. Signorelli, E. L. Coitiño, O. Borsani and J. Monza, *Molecular mechanisms for the*
51 *reaction between $\bullet OH$ radicals and proline: Insights on the role as reactive oxygen*
52 777 *species scavenger in plant stress, J. Phys. Chem. B*, 2014, **118**, 37–47.
53 778
54
55 779 89 A. Yadav and P. C. Mishra, *Modeling the activity of glutathione as a hydroxyl radical*
56
57
58
59
60

- 1
2
3 780 scavenger considering its neutral non-zwitterionic form, *J. Mol. Model.*, 2013, **19**, 767–
4 781 777.
- 5
6 782 90 J. Trembl and K. Smejkal, *Flavonoids as potent scavengers of hydroxyl radicals*, *Compr.*
7 783 *Rev. Food Sci. Food Saf.*, 2016, **15**, 720–738.
- 8
9 784 91 M. K. van Ittersum, L. G. J. van Bussel, J. Wolf, P. Grassini, J. van Wart, N. Guilpart, L.
10 785 Claessens, H. de Groot, K. Wiebe, D. Mason-D’Croz, H. Yang, H. Boogaard, P. A. J. van
11 786 Oort, M. P. van Loon, K. Saito, O. Adimo, S. Adjei-Nsiah, A. Agali, A. Bala, R. Chikowo,
12 787 K. Kaizzi, M. Kouressy, J. H. J. R. Makoi, K. Ouattara, K. Tesfaye and K. G. Cassman,
13 788 *Can sub-Saharan Africa feed itself?*, *Proc. Natl. Acad. Sci.*, 2016, **113**, 14964–14969.
- 14
15 789 92 P. Rengasamy, *World salinization with emphasis on Australia*, *J. Exp. Bot.*, 2006, **57**,
16 790 1017–1023.
- 17
18 791 93 S. Dasgupta, M. M. Hossain, M. Huq and D. Wheeler, *Climate change and soil salinity:*
19 792 *The case of coastal Bangladesh*, *Ambio*, 2015, **44**, 815–826.
- 20
21 793 94 J. Han, J. Shi, L. Zeng, J. Xu and L. Wu, *Effects of nitrogen fertilization on the acidity and*
22 794 *salinity of greenhouse soils*, *Environ. Sci. Pollut. Res.*, 2015, **22**, 2976–2986.
- 23
24 795 95 M. Qadir, E. Quill rou, V. Nangia, G. Murtaza, M. Singh, R. J. Thomas, P. Drechsel and
25 796 A. D. Noble, *Economics of salt-induced land degradation and restoration*, *Nat. Resour.*
26 797 *Forum*, 2014, **38**, 282–295.
- 27
28
29
30
31
32
33
34 798
35 799

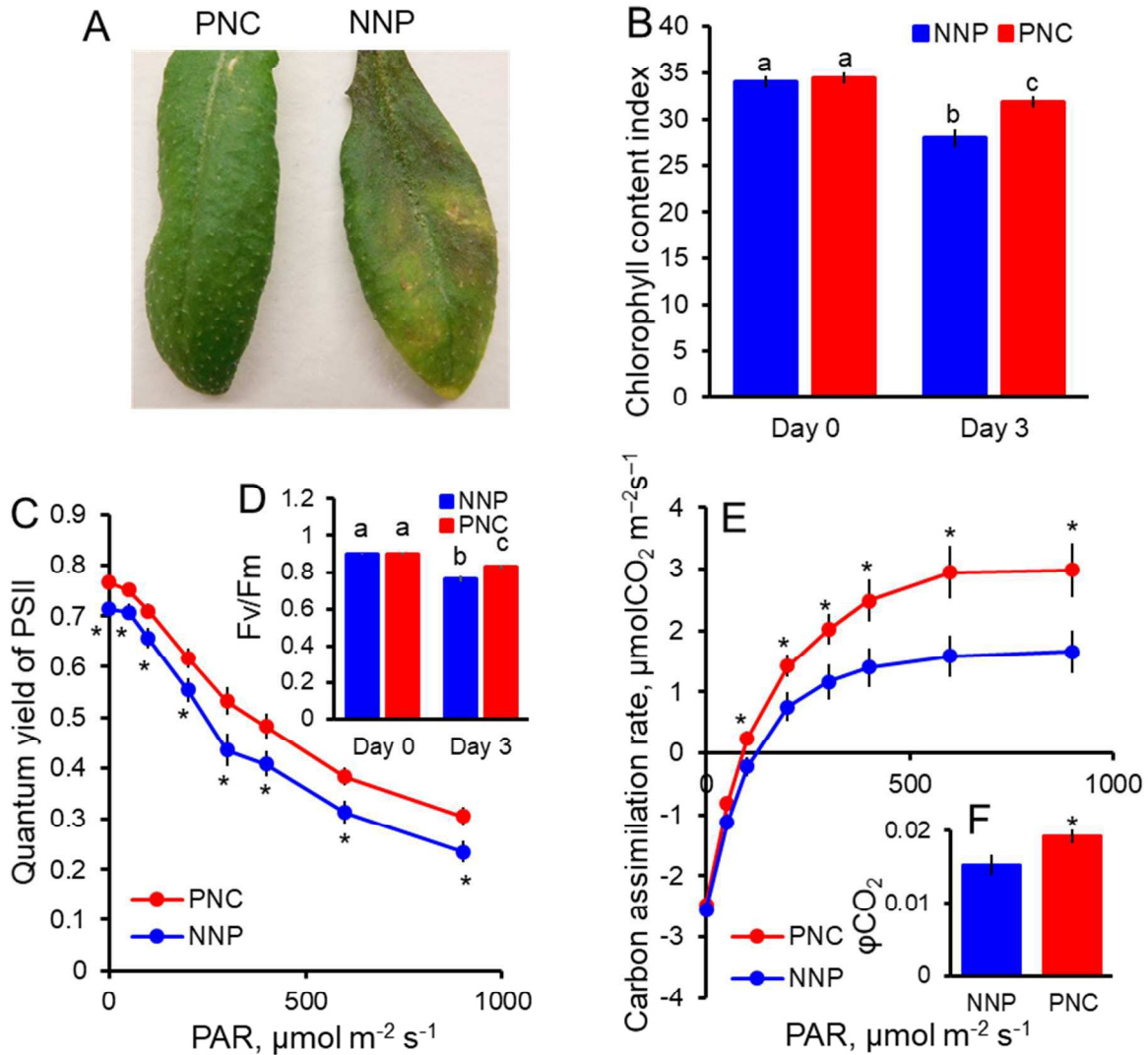
800 **Figure legends**801 **Figure 1**

802

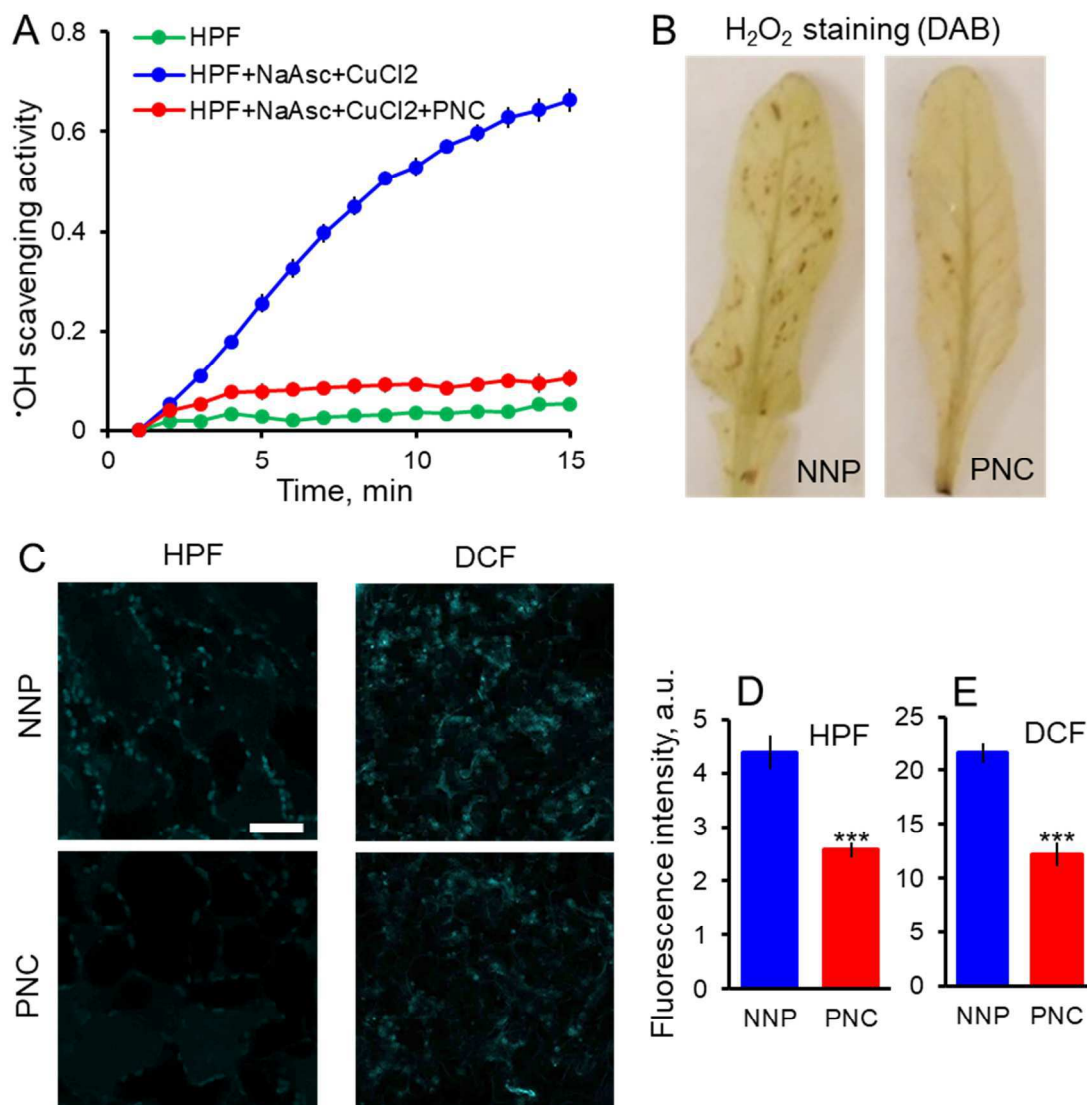
803 **Fig. 1** Model of nanoceria improvement of salt tolerance by enabling higher leaf mesophyll K⁺

804 retention. (A) Poly acrylic acid coated nanoceria (PNC, -17 mV, 10 nm) are delivered to

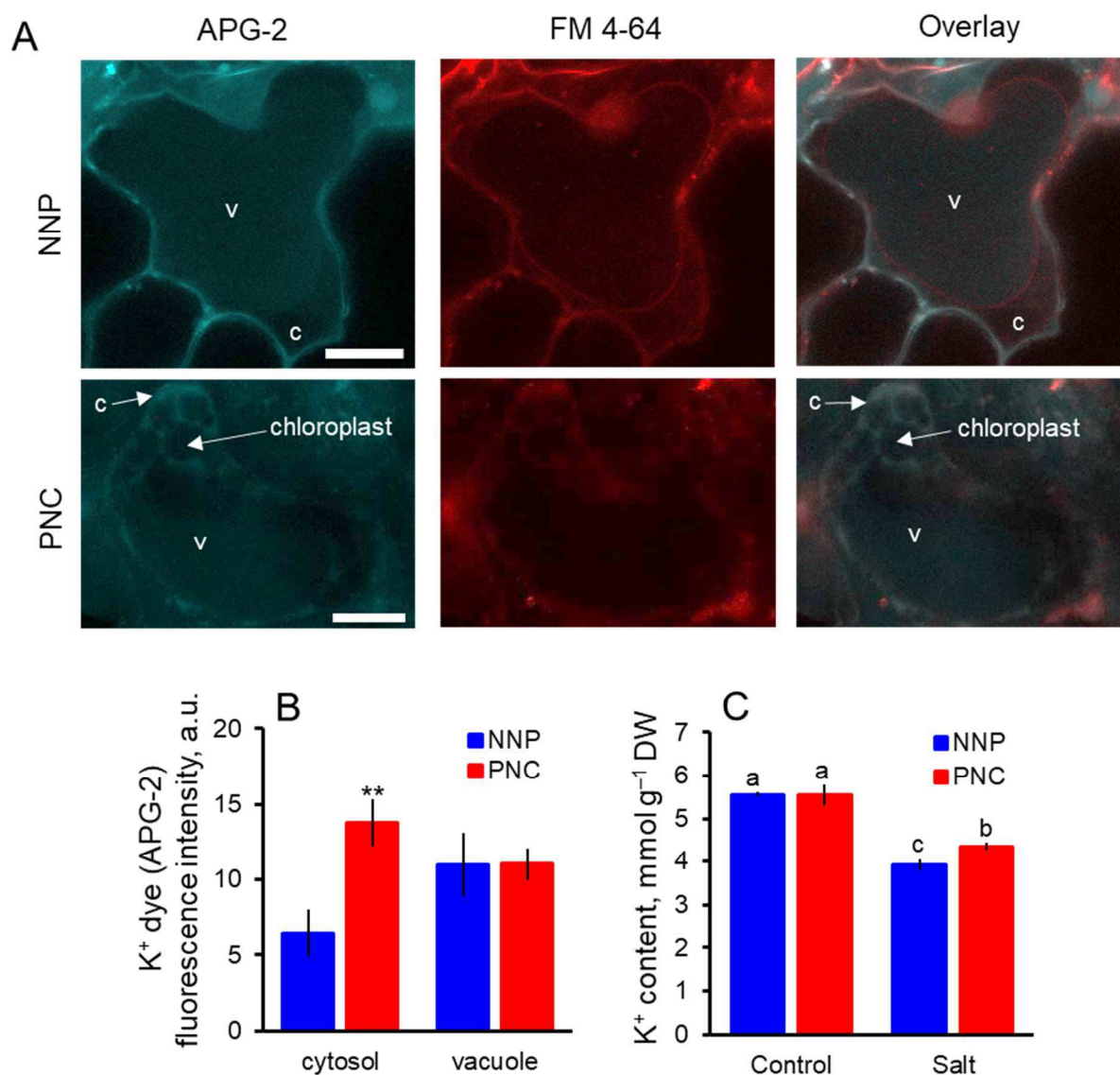
1
2
3 805 *Arabidopsis* leaf mesophyll cells through stomatal pores. **(B)** Nanoceria scavenging of hydroxyl
4 806 radicals ($\cdot\text{OH}$) and its precursor hydrogen peroxide (H_2O_2) influences mesophyll K^+ transport
5 807 under salt stress. Briefly, plant salt stress induces accumulation of ROS i.e $\cdot\text{OH}$ that activate
6 808 ROS-NSCC and GORK K^+ efflux channels. Large Na^+ influx into the cell cytosol also results in
7 809 GORK channel activation immediately after rapid plasma membrane potential depolarization.
8 810 However, once the plasma membrane potential is restored, the contribution to K^+ efflux
9 811 mediated by ROS has a larger impact than that induced by Na^+ influx. Nanoceria act as potent
10 812 catalytic scavengers of $\cdot\text{OH}$ and H_2O_2 alleviating oxidative stress and in turn reducing K^+ efflux
11 813 and improving K^+ retention. **(C)** PNC infiltrated *Arabidopsis* plants have higher salt tolerance
12 814 (100 mM NaCl, two weeks) than controls without nanoparticles. As, air space; Ep, epidermal cell;
13 815 G, guard cell.

816 **Figure 2**

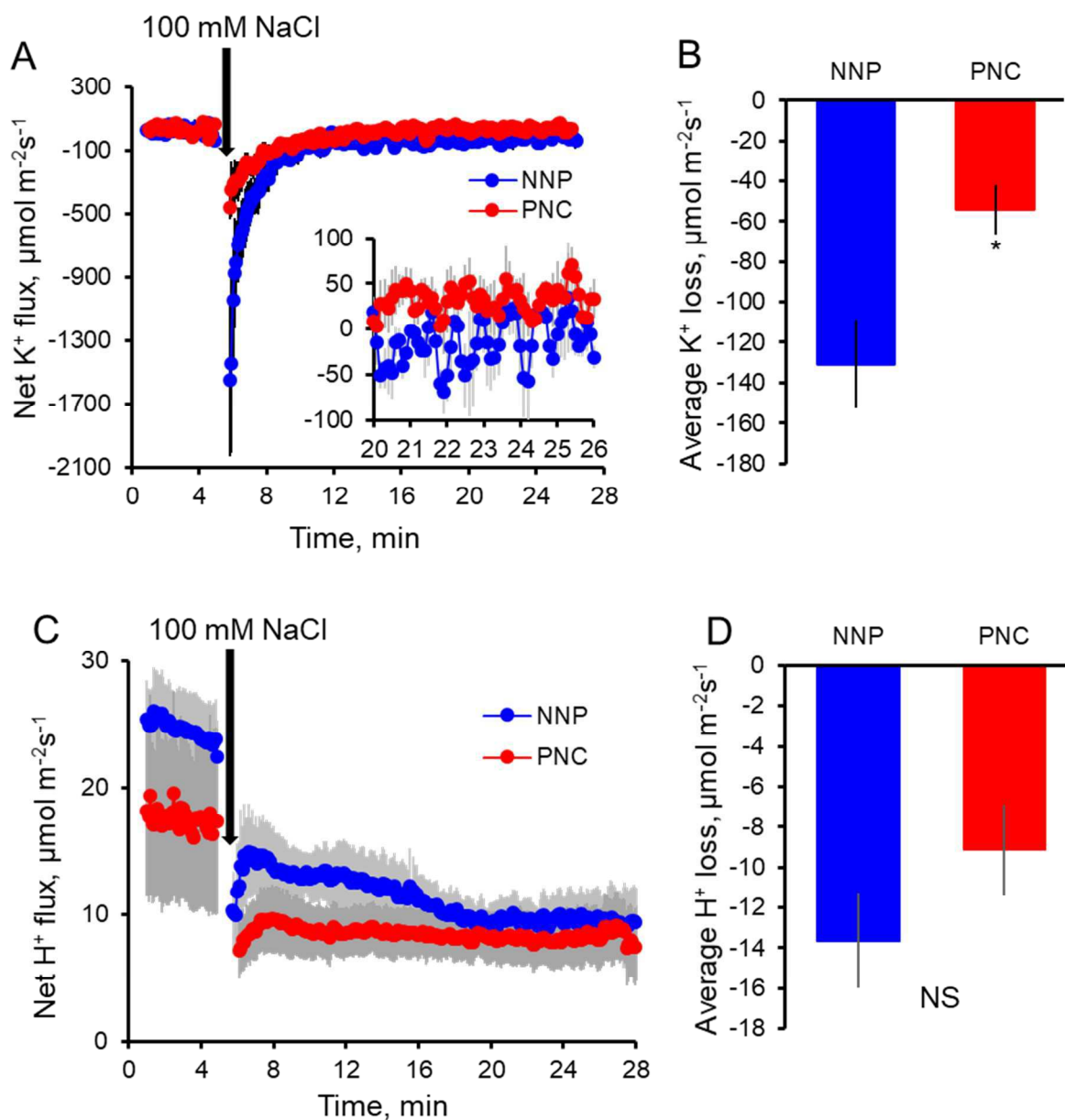
817
 818 **Fig. 2** Improved photosynthetic performance of leaves infiltrated with nanoceria in *Arabidopsis*
 819 plants exposed to salinity stress (100 mM NaCl, 3 days). (A and B) Comparison of chlorophyll
 820 content in leaves infiltrated with PNC (PNC-leaves) and buffer with no nanoparticles (NNP-
 821 leaves) at 0 and 3 days of exposure to 100 mM NaCl. Quantum yield of PS II (QY) (C),
 822 maximum quantum yield of PSII (Fv/Fm) (D), carbon assimilation rates (A) (E), and quantum
 823 efficiency of CO₂ (ϕCO_2) (F) of PNC-leaves and NNP-leaves after 3 days, 100 mM NaCl
 824 treatment. Mean \pm SE (n = 15-16). *, $P < 0.05$. Different lower case letters mean significant
 825 differences at $P < 0.05$.

826 **Figure 3**

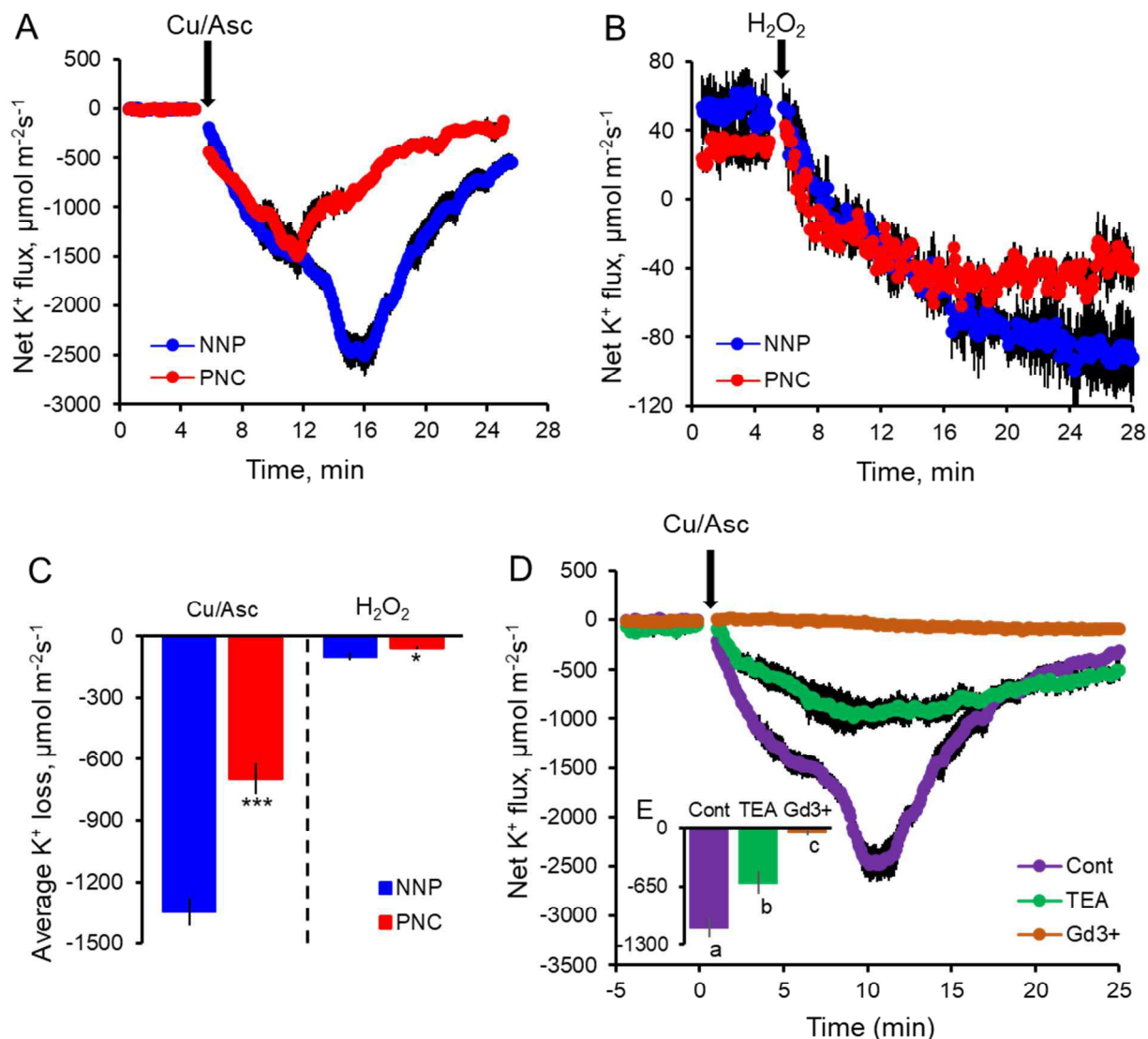
827
828 **Fig. 3** Catalytic scavenging of hydroxyl radical and hydrogen peroxide by nanoceria *in vitro* and
829 *in vivo* in *Arabidopsis* leaf mesophyll cells under salinity stress (100 mM NaCl, 3 days). (A)
830 PNC efficiently scavenges hydroxyl radicals generated by copper/ascorbate mixture. Hydroxyl
831 radicals were monitored by HPF fluorescent dye. Mean \pm SE (n = 3-6). (B) Histochemical
832 staining with DAB (hydrogen peroxide, dark brown spots) of leaves infiltrated with PNC (PNC-
833 Leaves) and buffer with no nanoparticles (NNP-Leaves) under salt stress. (C) Confocal images
834 of leaf spongy mesophyll cells showing the intensity of hydroxyl radical (HPF) and hydrogen
835 peroxide (DCF). (D and E), Comparison of HPF and DCF intensity between PNC-leaves and
836 NNP-leaves under salt stress. Mean \pm SE (n = 3-4). Scale bar represents 40 μ m. ***, $P < 0.001$.

837 **Figure 4**

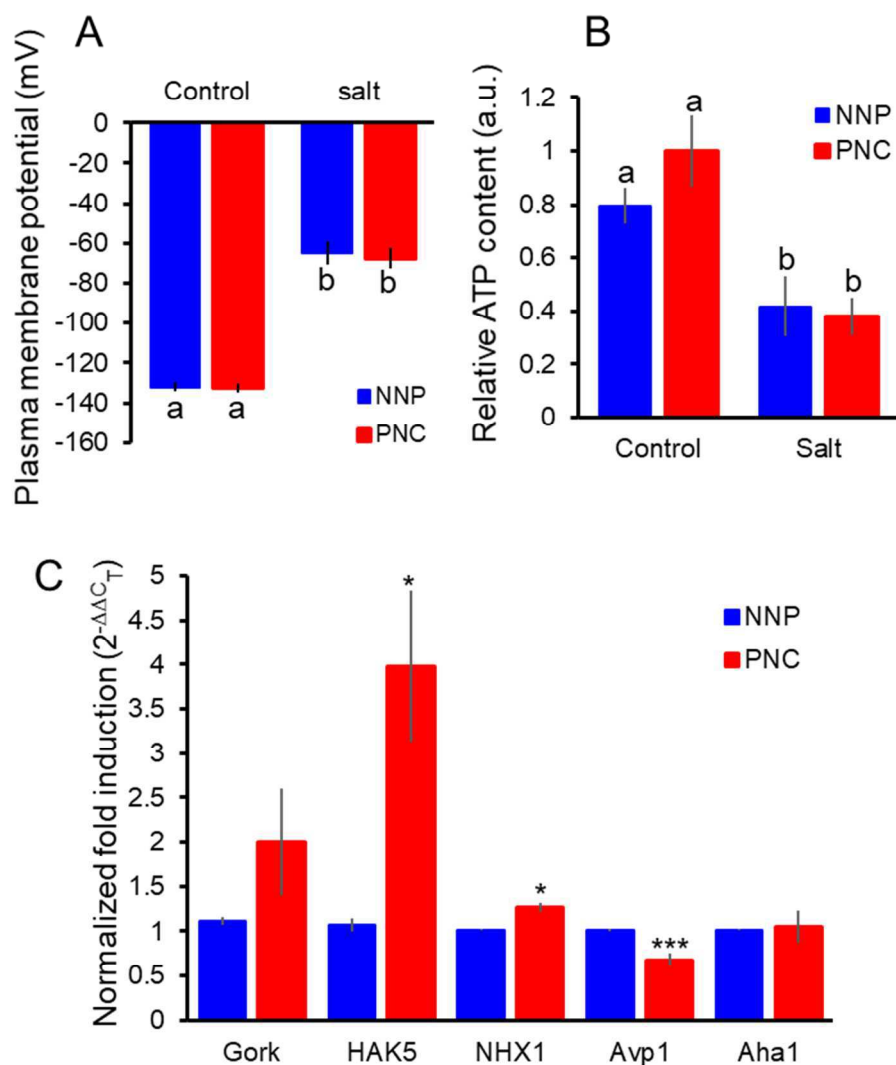
838
839 **Fig. 4** Higher cytosolic K⁺ retention ability in leaf mesophyll cells with embedded nanoceria
840 ROS scavengers in plants under salinity stress (100 mM NaCl, 3 days). (A) Confocal images of
841 K⁺ distribution in cytosol (c) and vacuole (v) measured by APG-2 dye in leaves infiltrated with
842 PNC (PNC-leaves) and buffer with no nanoparticles (NNP-leaves). The plasma membrane and
843 tonoplast were stained with FM 4-64. (B) Fluorescence intensity of APG-2 in cytosol and
844 vacuole. Mean ± SE (n = 4). (C) Leaf K⁺ content of PNC- and NNP-leaves under salt stress.
845 Mean ± SE (n = 5-6). Scale bar represents 20 μm. **, *P* < 0.01. Different lower case letters mean
846 significant differences at *P* < 0.05.

847 **Figure 5**

848
 849 **Fig. 5** Nanoceria ROS scavengers reduce leaf mesophyll K^+ efflux without affecting H^+ flux in
 850 plants under salt stress (100 mM NaCl, 3 days). NaCl-induced kinetics of mesophyll K^+ efflux
 851 (A), average K^+ loss (B), H^+ flux (C) and average H^+ loss (D) measured by MIFE in leaves
 852 infiltrated with PNC (PNC-leaves) and buffer with no nanoparticles (NNP-leaves). Mean \pm SE (n
 853 = 4-5). *, $P < 0.05$. NS, no significant difference.

854 **Figure 6**

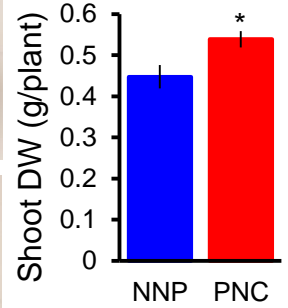
855
 856 **Fig. 6** Hydroxyl radical scavenging by nanoceria improves mesophyll K⁺ retention via NSCC
 857 channels. (A and B) Kinetics of mesophyll K⁺ efflux induced by hydroxyl radicals (generated by
 858 Cu/Asc, 0.3 mM/1 mM) and hydrogen peroxide (10 mM) in leaves infiltrated with PNC (PNC-
 859 leaves) and buffer with no nanoparticles (NNP). (C) Average K⁺ loss from mesophyll induced by
 860 hydroxyl radicals (generated by Cu/Asc mix) and hydrogen peroxide in leaves infiltrated with
 861 PNC (PNC-leaves) and buffer with no nanoparticles (NNP). (D and E) K⁺ efflux and average K⁺
 862 loss from leaf mesophyll in the presence of channel blocker of NSCC channels (Gd³⁺) and
 863 GORK channel inhibitor (TEA). Mean ± SE (n = 6-11). *, *P* < 0.05; ***, *P* < 0.001. Different
 864 lower case letters mean significant differences at *P* < 0.05.

865 **Figure 7**

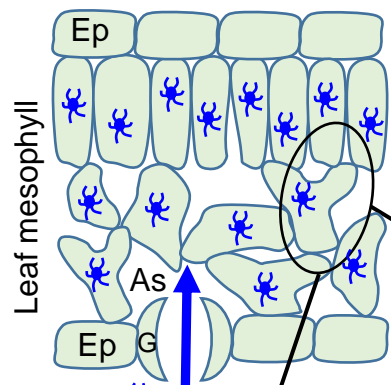
866
 867 **Fig. 7** Effect of PNC on plasma membrane potential, ATP content, and relative expression of K⁺
 868 channel/transporter genes in *Arabidopsis* leaves under salt stress. (A) Plasma membrane potential
 869 in leaves infiltrated with PNC and buffer with no nanoparticles (NNP) in response to salt stress.
 870 Mean ± SE (n = 5-7). (B) ATP content in PNC-leaves and NNP-leaves after salt stress. Mean ±
 871 SE (n = 4). (C) Relative expression of K⁺ channel/transporter genes in the plasma membrane and
 872 tonoplast of *Arabidopsis* leaves (Col-0) under 100 mM NaCl treatment for 3 days. Mean ± SE (n
 873 = 3). *, *P* < 0.05; ***, *P* < 0.001. Different lower case letters mean significant differences at *P* <
 874 0.05.

1
2
3
4
5
6
7
8
9
10
11
12
13
14
15
16
17
18
19
20
21
22
23
24
25
26
27
28
29
30
31
32
33
34
35
36
37
38
39
40
41
42
43
44
45
46
47
48
49
50
51
52
53
54
55
56

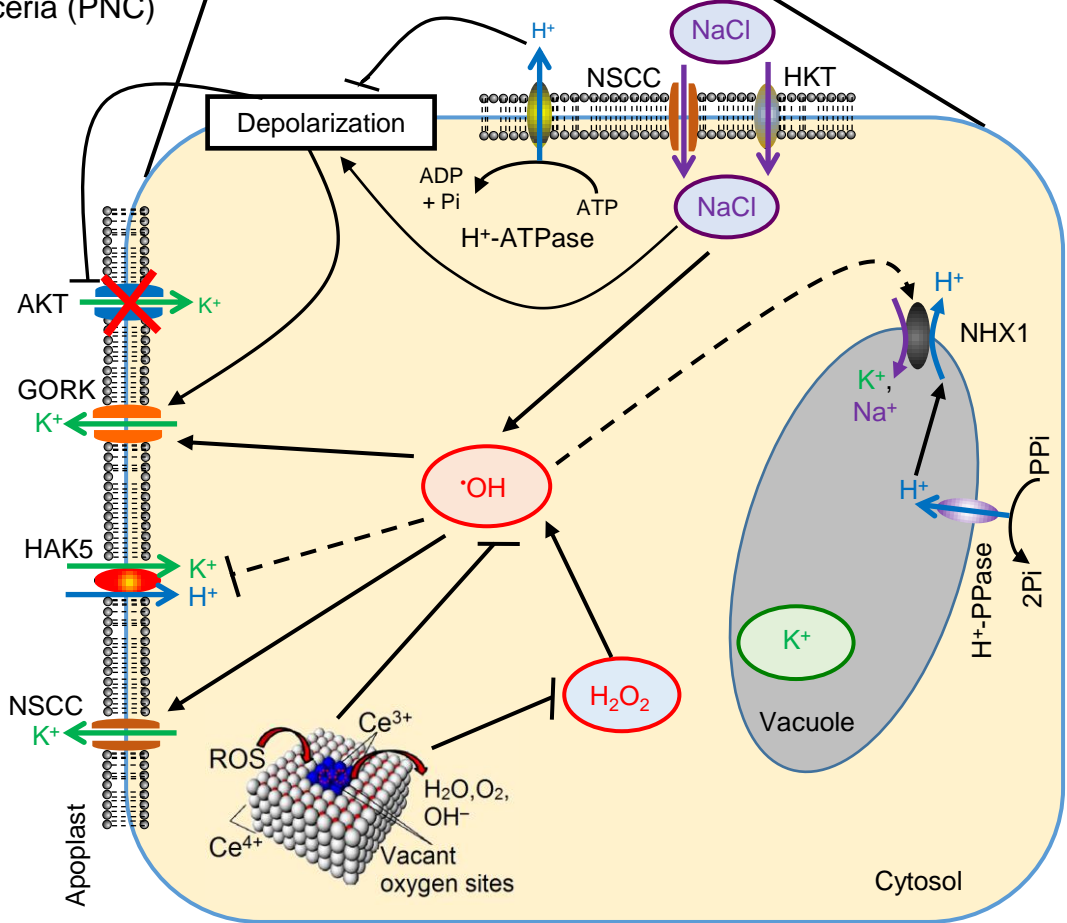
No nanoparticle control (NNP)



100 mM NaCl,
2 weeks



PAA-coated nanoceria (PNC)



→ Positive effect —| Negative effect - - - Proposed effect